Center for the Study of
Brain, Mind & Behavior

Optimizing reward rate in two alternative choice tasks: Mathematical formalism

Jeff Moehlis | Eric Brown

Rafal Bogacz | Philip Holmes

Jonathan D. Cohen

Center for the Study of Brain, Mind and Behavior
Princeton University
and
Program in Applied and Computational Mathematics
Department of Psychology
Department of Mechanical and Aerospace Engineering

Princeton University
Princeton, NJ 08544

Technical Report #04-01

Abstract

In this report we collect and summarize mathematical results and formalism appropriate to describing one-dimensional drift-diffusion processes (stochastic ordinary differential equations) and related first passage and probability density evolution problems, governed by the backward and forward Kolmogorov (Fokker-Planck) equations respectively. We start by reviewing the Neyman-Pearson and Sequential Probability Ratio tests as optimal strategies for choosing between two alternative hypotheses in the presence of accumulating, noisy data. The continuum analog of both of these tests is a constant drift-diffusion process, and we give direct proofs of optimality with respect to reward rate of such a process in the broader class of Ornstein-Uhlenbeck processes, both in terms of first passages and density evolution. These correspond to the free response and interrogation protocols used in psychological testing. We end by considering the effects of variable gain on selected inputs to drift-diffusion and Ornstein-Uhlenbeck processes, and deriving optimal gain schedules for time-varying signal-to-noise ratios. Parts of this report are an extended version of the appendix to [1]; others appear in the paper [2].

1 Introduction

There is a substantial literature in psychology on drift-diffusion processes as models for simple decision making, especially in two-alternative forced-choice (TAFC) tasks. Laming's text [3] introduced the 'random walk model' of choice reaction times, although Stone [4] had earlier applied a statistical procedure, the sequential probability ratio test, to the interpretation of behavioral data. Ratcliff [5] and Ratcliff et al. [6] provide more recent examples and critical reviews. The models are discussed in a largely phenomenological manner: parameter fitting to individual subjects allows accurate reproduction of reaction time distributions and error rates, and accounts for more subtle effects, but how the drift-diffusion process is realised at the neural level is not addressed.

However, recent *in vivo* recordings in behaving primates (e.g. [7]), as well as growing evidence from functional magnetic resonance imaging (fMRI) on human subjects, suggest that certain groups of neurons (e.g. in monkey lateral interparietal area and frontal eye fields) integrate incoming stimuli in that their mean firing rates increase (approximately linearly) until a threshold is reached and a decision is made, signalled, for example, by saccade initiation. These data are very suggestive of drift-diffusion dynamics. (Various mechanisms for neural integration have been proposed, e.g. [8, 9, 10].) At the same time, several authors have suggested that optimal decision making ideas from information theory and statistical decision theory may provide a guide to neural realizations [11, 12, 13, 14]. It is therefore useful to review some key properties of drift-diffusion and related models, and to analyse them in more explicit detail than appears to have been done previously. For example, while a numerically generated plot of reward rate versus threshold, similar to (the inverse of) Figure 1 below, appears in [13], to our knowledge explicit formulae have not previously been published.

In this report we collect and describe mathematical details necessary for solution of first passage and boundaryless drift-diffusion problems. We consider both pure (constant and time-dependent) drift and Ornstein-Uhlenbeck processes. The main tools are simple notions from applied probability, the theory of stochastic ordinary differential equations, and classical perturbation and asymptotic methods. Much of the earlier work centered on discrete random walk models, and while exact solutions are available, they are frequently awkward expressions involving infinite sums (cf. Feller [15, Chapter XIV]). Here we focus on continuous models in the form of stochastic ordinary differential equations, although we first describe how these arise as limits of a discrete statistical process: the sequential probability ratio test, which is the optimal method of deciding between two alternatives on the basis of noisy accumulating data. It turns out that the optimal continuous processes admit rather simple exact formulae for such behavioral observables as mean reaction times and error rates.

Section 2 reviews the classical probability ratio (or maximum likelihood) test, and the sequential probability ratio test, and describes how it becomes a drift diffusion process in the continuum limit. Sections 3 considers the free response protocol, in which subjects make choices in their own time, and Section 4 addresses the interrogation protocol, in which a decision is deferred until a cue is presented. The report ends with a discussion of optimal strategies for varying gain in the presence of data whose signal-to-noise ratio varies with time.

2 Probability Ratio Tests

Suppose we wish to decide whether a random sequence $Y = y_1, y_2, \cdots, y_N$ of N independent observations is drawn from the probability distribution $p_0(y)$ (hypothesis H_0) or $p_1(y)$ (hypothesis H_1). Neyman and Pearson [16] showed that the optimal procedure is to calculate

$$\frac{p_{1N}}{p_{0N}} = \frac{p_1(y_1)p_1(y_2)\cdots p_1(y_N)}{p_0(y_1)p_0(y_2)\cdots p_0(y_N)}\,, \tag{1}$$

and to accept hypothesis H_0 (resp., H_1) if $\frac{p_{1N}}{p_{0N}} < K$ (resp., $\frac{p_{1N}}{p_{0N}} \geq K$), where K is a constant determined by the desired level of accuracy for one of the hypotheses. Setting $K < 1$ increases the reliability of the decision to accept H_0, at the expense of reducing the reliability of accepting H_1. Since the p_{iN}, $i = 0, 1$ are the probabilities of Y occurring under the hypotheses H_i, setting $K = 1$ reduces the procedure to simply determining which hypothesis is most likely (determining 'maximum likelihood'). In this case, if the hypotheses occur with equal probability, the procedure guarantees the smallest overall error rate.

However, the Neyman-Pearson procedure is only optimal when the sequence size N is *fixed* in advance; when this requirement is relaxed, the optimal procedure is the *sequential probability ratio test*, hereafter denoted SPRT. Here A_0 and A_1 are two given constants, and observations continue as long as $\frac{p_{1n}}{p_{0n}}$ satisfies the inequality

$$A_0 < \frac{p_{1n}}{p_{0n}} < A_1\,. \tag{2}$$

The hypothesis H_0 (resp., H_1) is accepted at step n as soon as $\frac{p_{1n}}{p_{0n}} \leq A_0$ (resp., $\frac{p_{1n}}{p_{0n}} \geq A_1$). The SPRT was independently developed during World War II by Abraham Wald [17], who was introduced to the problem by Milton Friedman and W. Allen Wallis while all were members of the Statistical Research Group at Columbia University [18], and by George Barnard [19, 20] in Great Britain. Furthermore, Alan Turing and coworkers at Bletchley Park employed the SPRT to break the Enigma code used by the German navy in World War II [21, 13]. Sadly, both Wald and Turing died prematurely: Wald died in a plane crash *en route* to a scientific presentation in India in 1950, and Turing (apparently) committed suicide in 1954. The field of sequential analysis, invigorated by the SPRT, has continued to develop as a very active research area: see, e.g., [22, 23, 24, 25, 26, 27]; also, see [26] for more on the history of the SPRT.

2.1 Optimality of the sequential probability ratio test

The SPRT is optimal in the following sense. Let $P(\text{rej H}_i|\text{H}_i)$ be the probability that hypothesis H_i is true but rejected, $i = 0, 1$. Also, let $E_i(N)$ be the expected value for the number of observations required for a decision to be reached when hypothesis H_i is true, $i = 0, 1$. We then have the following theorem first proved in [28]; here we sketch the simpler proof given in [29], cf. [22].

> **SPRT Optimality Theorem:** Among all tests (fixed sample or sequential) for which
>
> $$P(\text{rej H}_i|\text{H}_i) \leq \alpha_i, \qquad i = 0, 1,$$
>
> and for which $E_0(N)$ and $E_1(N)$ are finite, the SPRT with error probabilities $P(\text{rej H}_i|\text{H}_i) = \alpha_i$, $i = 0, 1$, minimizes both $E_0(N)$ and $E_1(N)$.

Sketch of Proof. The proof involves solving the following auxiliary problem. Let w_0 (resp., w_1) be the loss associated with choosing H_1 when H_0 is true (resp., choosing H_0 when H_1 is true). Furthermore, let c be the cost associated with each observation. When H_i holds, the risk R_i is defined to be the sum of the expected loss due to an incorrect decision and the expected cost:

$$R_i = \alpha_i w_i + cE_i(N), \qquad i = 0, 1.$$

Finally, suppose that a large number of trials are considered, and H_1 (resp., H_0) is true with probability Π (resp., $1 - \Pi$). (Note that we adopt the opposite convention to that of [29, pp. 104-110].) The total average risk associated with a decision procedure δ is then

$$r(\Pi, c, w_0, w_1, \delta) = (1 - \Pi)R_0 + \Pi R_1 = (1 - \Pi)[\alpha_0 w_0 + cE_0(N)] + \Pi[\alpha_1 w_1 + cE_1(N)]\,. \qquad (3)$$

The proof proceeds by showing that the SPRT minimizes $r(\Pi, c, w_0, w_1, \delta)$ in the following sense: given any SPRT with $A_0 < 1 < A_1$ (the specific values of A_0 and A_1 determine the error rates α_0 and α_1, see below) and any $0 < \Pi < 1$, there exist positive constants c, w_0 and w_1 such that the SPRT minimizes $r(\Pi, c, w_0, w_1, \delta)$ for those values of Π, c, w_0, and w_1. We refer the reader to [29, 22] for details of this argument. Now, let δ^* be a different decision procedure with error probabilities $\alpha_i^* \leq \alpha_i$, and finite expected sample sizes $E_i^*(N)$, $i = 0, 1$. Then

$$r(\Pi, c, w_0, w_1, \delta^*) = (1 - \Pi)[\alpha_0^* w_0 + cE_0^*(N)] + \Pi[\alpha_1^* w_1 + cE_1^*(N)]\,.$$

From the above, we know that for any $0 < \Pi < 1$, we can choose specific (positive) values of c, w_0, and w_1 such that

$$r(\Pi, c, w_0, w_1, \delta) \leq r(\Pi, c, w_0, w_1, \delta^*),$$

that is,

$$\begin{aligned}(1 - \Pi)[\alpha_0 w_0 + cE_0(N)] + \Pi[\alpha_1 w_1 + cE_1(N)] &\leq (1 - \Pi)[\alpha_0^* w_0 + cE_0^*(N)] + \Pi[\alpha_1^* w_1 + cE_1^*(N)] \\ &\leq (1 - \Pi)[\alpha_0 w_0 + cE_0^*(N)] + \Pi[\alpha_1 w_1 + cE_1^*(N)]\,.\end{aligned}$$

Thus,

$$(1-\Pi)E_0(N) + \Pi E_1(N) \leq (1-\Pi)E_0^*(N) + \Pi E_1^*(N)\,.$$

Since this is valid for any Π, we conclude that

$$E_0(N) \leq E_0^*(N), \qquad E_1(N) \leq E_1^*(N)\,. \qquad \square$$

The constants A_0 and A_1 in the SPRT are related to the error rates α_0 and α_1 as follows [17, 29]. Consider the set C_1 of n-length sequences Y such that the SPRT chooses H_1 when Y occurs. That is, for any $Y \in C_1$,

$$p_1(y_1)p_1(y_2)\cdots p_1(y_n) \geq A_1 p_0(y_1)p_0(y_2)\cdots p_0(y_n).$$

Integrating this inequality over all of C_1,

$$p_1(C_1) \geq A_1 p_0(C_1), \tag{4}$$

where $p_j(C_1)$ is the probability of making choice 1 given that hypothesis H_j is true. By definition, $p_1(C_1) \geq 1-\alpha_1$ and $p_1(C_0) \leq \alpha_0$, so that

$$1-\alpha_1 \geq A_1\alpha_0 \qquad \Rightarrow \qquad A_1 \leq \frac{1-\alpha_1}{\alpha_0}.$$

Similarly,

$$\alpha_1 \leq A_0(1-\alpha_0) \qquad \Rightarrow \qquad A_0 \geq \frac{\alpha_1}{1-\alpha_0}.$$

The inequalities fail to be equalities because it is possible to overshoot the boundaries A_0 or A_1. However, in practice, there is typically little penalty in assuming equality [17, 29]:

$$A_0 = \frac{\alpha_1}{1-\alpha_0}, \qquad A_1 = \frac{1-\alpha_1}{\alpha_0}. \tag{5}$$

Note that, when using an SPRT with A_0 and A_1 defined in this way, the condition that $A_0 < 1 < A_1$ in the proof becomes

$$\frac{\alpha_1}{1-\alpha_0} < 1 < \frac{1-\alpha_1}{\alpha_0}. \tag{6}$$

Thus, the proof requires that $\alpha_1 < 1-\alpha_0$. Now, $1-\alpha_0$ is the probability of choosing H_0 when H_0 is true. Thus, the proof requires that the probability of choosing H_0 when H_1 is true is less than the probability of choosing H_0 when H_0 is true. Similarly, it requires that $\alpha_0 < 1-\alpha_1$, that is, the probability of choosing H_1 when H_0 is true is less than the probability of choosing H_1 when H_1 is true. These are, of course, very reasonable conditions for a decision making procedure. Wald [17] also gives approximate expressions for the expected numbers of observations $E_i(N)$. Using (5), these may be written

$$E_1(N) \approx \frac{\alpha_1 \log\left(\frac{\alpha_1}{1-\alpha_0}\right) + (1-\alpha_1)\log\left(\frac{1-\alpha_1}{\alpha_0}\right)}{E_1\left(\log\left(\frac{p_1(y)}{p_0(y)}\right)\right)} \tag{7}$$

$$E_0(N) \approx \frac{(1-\alpha_0)\log\left(\frac{\alpha_1}{1-\alpha_0}\right) + \alpha_0\log\left(\frac{1-\alpha_1}{\alpha_0}\right)}{E_0\left(\log\left(\frac{p_1(y)}{p_0(y)}\right)\right)}, \tag{8}$$

where $E_i\left(\log\left(\frac{p_1(y)}{p_0(y)}\right)\right)$ is the expected value of the argument when H_i is true, $i = 0, 1$.

We also note that the proof in [29] applies to the generalized case of decisions based on biased data. Suppose that the subject has been told (or has deduced) that the probability of drawing from the distribution $p_1(y)$ (resp. $p_0(y)$) is Π (resp., $1 - \Pi$). Then the SPRT continues as long as

$$A_0 < \frac{\Pi p_{1n}}{(1-\Pi)p_{0n}} < A_1.$$

Equivalently, the thresholds A_j are simply multiplied by $(1 - \Pi)/\Pi$; i.e., observations are taken as long as:

$$\frac{1-\Pi}{\Pi} A_0 < \frac{p_{1n}}{p_{0n}} < \frac{1-\Pi}{\Pi} A_1 \,. \tag{9}$$

Thus if the 'upper' alternative is more probable ($\Pi > 1/2$) both thresholds are shifted down, and vice versa.

2.2 The sequential probability ratio test optimizes reward rate

Modestly extending the SPRT Optimality Theorem stated above, we now show that the procedure also optimizes the reward rate introduced in [13]. This requires allowing error rates to vary as well as seeking to minimize the number of observations required.

As above, we define the error rates (assumed equal) to be

$$\mathrm{ER} = P(\text{rej } \mathrm{H}_0|\mathrm{H}_0) = P(\text{rej } \mathrm{H}_1|\mathrm{H}_1) = \epsilon \,,$$

and the mean reaction time RT to be the average time needed to make a decision. Furthermore, we define the reward rate RR to be the probability of a correct response divided by the average time between responses. Allowing an imposed delay $D \geq 0$ between trials and an additional penalty delay $D_p \geq 0$ after incorrect responses, this is:

$$\mathrm{RR} = \frac{1 - \mathrm{ER}}{\mathrm{RT} + D + D_p \mathrm{ER}} \,. \tag{10}$$

For a given decision procedure δ^*, suppose that RR is maximized for $\mathrm{ER} = \epsilon^*$. (Determining ϵ^* may be difficult in practice, because different values for ER generally correspond to different values for RT.) Now, consider the SPRT δ with $\mathrm{ER} = \epsilon^*$. From the SPRT Optimality Theorem, $\mathrm{RT}(\delta, \epsilon^*) \leq \mathrm{RT}(\delta^*, \epsilon^*)$. Thus,

$$\begin{aligned} \mathrm{RR}(\delta^*, \epsilon^*) &= \frac{1 - \epsilon^*}{\mathrm{RT}(\delta^*, \epsilon^*) + D + D_p \epsilon^*} \\ &\leq \frac{1 - \epsilon^*}{\mathrm{RT}(\delta, \epsilon^*) + D + D_p \epsilon^*} = \mathrm{RR}(\delta, \epsilon^*) \,; \end{aligned}$$

that is, one can always find an SPRT which yields a reward rate at least as high as that obtained from the decision procedure δ^*. Furthermore, there will be a particular value of ϵ which gives the SPRT (and hence the decision procedure) with the largest possible reward rate. This ϵ will also be difficult to determine in practice because different values for ER generally correspond to different values from RT: see below. Note that ϵ sets the decision thresholds of the random walk model (cf. (13)). Thus, in the next section, we will be particularly interested in determining the thresholds for our constant drift-diffusion equation which give the highest possible reward rate.

2.3 Random walks and the continuum limit

Following [4], Laming applies the SPRT to a two-alternative forced-choice task in [3]. In such a task, on each trial a randomly chosen stimulus $\mathcal{S}_0$ or $\mathcal{S}_1$ is shown to the subject. The subject is told to give a response $\mathcal{R}_i$ if he or she perceives stimulus $\mathcal{S}_i$, $i = 0, 1$. The response made (which may or may not be correct) and the reaction time (RT) taken to make it are recorded for each trial.

Laming models this procedure by supposing that decisions are made based on accumulation of information. Specifically, for each trial the subject makes a series of brief observations of the stimulus represented by the random sequence $y_1, y_2, \cdots, y_n$. The increment of information gained from (independent) observation y_r is defined to be

$$\delta I_r = \log\left(\frac{p_1(y_r)}{p_0(y_r)}\right), \tag{11}$$

or the 'log likelihood ratio' [12, 13], where $p_i(y)$ is the probability distribution for y given that stimulus $\mathcal{S}_i$ was presented, $i = 0, 1$. (Implicitly, the subject has some internal representation of $p_0(y)$ and $p_1(y)$.) At the n^{th} observation, the total information accumulated is

$$I_n = \sum_{r=1}^{n} \delta I_r = \sum_{r=1}^{n} \log\left(\frac{p_1(y_r)}{p_0(y_r)}\right). \tag{12}$$

Observations continue as long as $\mathcal{I}_0 < I_n < \mathcal{I}_1$, where $\mathcal{I}_0$ and $\mathcal{I}_1$ are constants. The response $\mathcal{R}_0$ (resp., $\mathcal{R}_1$) is made at step n if $I_n \le \mathcal{I}_0$ (resp., $I_n \ge \mathcal{I}_1$). Since, from (1),

$$I_n = \log\left(\frac{p_{1n}}{p_{0n}}\right),$$

we see that the accumulation of information according to this formulation is equivalent to making decisions using the SPRT with $\mathcal{I}_0 = \log A_0$ and $\mathcal{I}_1 = \log A_1$, cf. [17, 13]. For example, if the desired error rates are $\alpha_0 = \alpha_1 = \epsilon$, which is reasonable if the signals $\mathcal{S}_0$ and $\mathcal{S}_1$ are equally salient, from (5) we take

$$\mathcal{I}_0 = \log\left(\frac{\epsilon}{1-\epsilon}\right) < 0, \qquad \mathcal{I}_1 = \log\left(\frac{1-\epsilon}{\epsilon}\right) = -\mathcal{I}_0 > 0, \tag{13}$$

cf. [3]. (The signs follow from the assumed inequality (6).) If we require equal error rates in the case of signals of unequal salience, with Π denoting the probability of $\mathcal{S}_1$, then multiplying the boundaries of (5) and taking logs we find:

$$\mathcal{I}_0 = \log\left(\frac{1-\Pi}{\Pi}\right) + \log\left(\frac{\epsilon}{1-\epsilon}\right), \qquad \mathcal{I}_1 = \log\left(\frac{1-\Pi}{\Pi}\right) + \log\left(\frac{1-\epsilon}{\epsilon}\right). \tag{14}$$

To maintain $\mathcal{I}_0 < 0 < \mathcal{I}_1$ we must select an error rate lower than the smaller of Π and $1 - \Pi$.

Thus, from (12), in logarithmic variables the trajectory I_n is a discrete-time, biased random walk with initial condition zero: a new increment of information arrives, and the trajectory is updated, as the timestep advances from $n \to n + 1$ (recall that the increments δI_r are assumed to be independent and identically distributed). Hereafter we treat the continuous-time limit

$I(t)$ of this process, in which infinitesimal increments of information arrive at each moment in time (see references in [29]). This limit must be taken with some care in order to preserve the variability present in (12). Up to an unimportant scale factor between 'timesteps' n and the continuous time t, the limiting procedure is as follows. Let the δI_r have mean m and variance D^2 (assumed finite). Then define the family (indexed by $N = 1, 2, ...$) of random functions of $t \in [0, T]$, where T is some large time, as follows:

$$I^N(t) = \frac{1}{\sqrt{N}} \sum_{r=1}^{k} (\delta I_r - m) + \frac{1}{N} \sum_{r=1}^{k} \delta I_r \,, \quad \text{where} \quad k = \lfloor Nt/T \rfloor \,. \tag{15}$$

Here, $\lfloor Nt/T \rfloor$ is the largest integer smaller than Nt/T. Note that the first term of (15) is normalized by $1/\sqrt{N}$ and the second by by $1/N$, reflecting the different rates at which fluctuations and means accumulate as the random increments are summed. For *any* N, $I^N(t)$ has mean $m\lfloor t/T \rfloor$ and variance $D^2 \lfloor t/T \rfloor$; e.g., from (12), I_n has mean mn and variance $D^2 n$. Furthermore, the Donsker Invariance Principle (see Thm. 37.8 of [30]), together with the Law of Large Numbers, implies that as $N \to \infty$

$$I^N(t) \Rightarrow D\,W(t) + mt \equiv I(t) \ \ , \tag{16}$$

where $W(\cdot)$ is a Wiener process (see below) and the convergence of the random functions $I^N(\cdot)$ is in the sense of distributions. In other words, the limiting process $I(t)$ satisfies the stochastic differential equation

$$dI = m\,dt + D\,dW \,, \quad I(0) = 0 \,, \tag{17}$$

with boundaries $\mathcal{I}_0 < 0 < \mathcal{I}_1$. The drift m and variance D of the δI_r and hence of (17) depend upon the distributions $p_i(y)$, cf. (11). For example, in the case of Gaussians

$$p_0(y) = \frac{1}{\sqrt{2\pi\sigma^2}}\, e^{-(y-\mu_0)^2/(2\sigma^2)} \,, \quad p_1(y) = \frac{1}{\sqrt{2\pi\sigma^2}}\, e^{-(y-\mu_1)^2/(2\sigma^2)} \,, \tag{18}$$

with $\mu_1 > \mu_0$, we have

$$\delta I_r = \log\left(\frac{p_1(y_r)}{p_0(y_r)}\right) = \frac{\mu_1 - \mu_0}{\sigma^2}\left(y_r - \frac{\mu_0 + \mu_1}{2}\right) \,, \tag{19}$$

and if $\mathcal{S}_i$ is presented, the expected value of y_r is $E(y_r) = \mu_i$, and the variance is $Var(y_r) = \sigma^2$. Thus, taking expectations and substituting in (19), we obtain

$$E(\delta I_r) = \pm \frac{(\mu_1 - \mu_0)^2}{2\sigma^2} = m, \tag{20}$$

(the + applies if $\mathcal{S}_1$ is presented, the $-$ if $\mathcal{S}_0$), and in both cases

$$Var(\delta I_r) = \mu_1 - \mu_0 = D^2, \tag{21}$$

cf. [12, 13]. If each incremental observation δI_r is composed of many subobservations (for example, from different regions of the visual field, or from large populations of neurons), this Gaussian assumption is justified by the Central Limit Theorem.

In the particular case of (19) in which $\mu_1 = -\mu_0 = A$, $\sigma = c$, appropriate to tasks such as the 'moving dots' paradigm in which the alternative stimuli are of equal clarity (e.g. [7]), the simplified form of (19) implies that the accumulating information I_n is simply a scaled version of the running total of observations y_r:

$$\delta I_r = \frac{2A}{c^2} y_r \Rightarrow I_n = \sum_{r=1}^{n} \delta I_r = \frac{2A}{c^2} \sum_{r=1}^{n} y_r \stackrel{\text{def}}{=} \frac{2A}{c^2} y_n \,. \tag{22}$$

Assuming without loss of generality that $\mathcal{S}_1$ is presented, the y_r have mean A (and variance c^2) so that, in the continuous time limit analogous to (15), y_n converges to $y(t)$, which satisfies the drift-diffusion stochastic differential equation:

$$dy = A\,dt + c\,dW \,; \quad y(0) = 0 \,. \tag{23}$$

The 'logarithmic' SPRT involving observations δI_r is therefore equivalent to solving the first passage problem defined by (23) with thresholds $y = z_1 = \frac{c^2}{2A} \mathcal{I}_i$, and $\mathcal{I}_i$ as in (13-14).

In the event of unequal salience ($\Pi \neq 1/2$), rather than employing the asymmetric boundaries of (14) we may transform by letting $y \mapsto y + \frac{c^2}{2A} \log\left(\frac{\Pi}{1-\Pi}\right)$, and consider the process (17) with biased initial data

$$y(0) = \frac{c^2}{2A} \log\left(\frac{\Pi}{1-\Pi}\right) \tag{24}$$

and symmetric boundaries

$$-z < 0 < z = \frac{c^2}{2A} \log\left(\frac{1-\epsilon}{\epsilon}\right) \,. \tag{25}$$

Thus, when $\Pi \neq 1/2$, the process starts closer to the threshold corresponding to the more probable alternative. We study these and more general drift-diffusion problems in the following sections.

We emphasize that the constant drift stochastic differential equation (17) or (23) is a particular limit of the discrete random walk occurring in the SPRT or Neyman-Pearson tests, and that more general stochastic differential equations, such as Ornstein-Uhlenbeck processes, correspond to other (i.e. non-optimal) decision strategies. In the following sections we analyse these stochastic processes in both unconstrained (free response) and time-constrained (interrogation) contexts.

3 Optimal Decisions for the Free Response Protocol

As suggested by the above discussion, we model the decision-making process for the two-alternative forced-choice task as a one-dimensional drift-diffusion process on the x-axis with two (symmetric) thresholds $x = \pm z$. The drift term represents the weight of evidence in favor of one alternative; diffusion arises from unmodelled inputs, represented as white noise. We consider constant and linear (Ornstein-Uhlenbeck) drift processes, both of which arise naturally in connectionist models of such tasks [1]. In the free response protocol, in which subjects are free to respond at any time after stimulus onset, we assume that a decision is made when the sample path first crosses either threshold; thus, we have a first passage problem. Here we summarize the derivation of the probabilities of first passages through the thresholds, and of first passage times to either threshold, from the backward Kolmogorov or Fokker-Planck equation. These in turn represent expected error and %-correct rates and mean reaction times. We also derive expressions for the reward rate for these processes, and show explicitly that the constant drift process allows higher reward rates than are possible from an Ornstein-Uhlenbeck process.

3.1 General considerations

Suppose we have the stochastic differential equation

$$dx = g(x)\,dt + \sqrt{D(x)}\,dW\,, \tag{26}$$

where (first) passage of the trajectory through $x = a$ (resp., $x = b$) corresponds to an incorrect (resp., correct) decision. Here $W(t)$ is a standard Wiener process. Recall that a standard Wiener process (often called Brownian motion) on the interval $[0, T]$ is a random variable $W(t)$ that depends continuously on $t \in [0, T]$ and satisfies the following [31, 32]:

- $W(0) = 0$.
- For $0 \leq s < t \leq T$,
$$W(t) - W(s) \sim \sqrt{t-s}N(0, 1)\,,$$
where $N(0, 1)$ is a normal distribution with zero mean and unit variance. Therefore, the process is often referred to as Gaussian.
- For $0 \leq s < t < u < v \leq T$, $W(t) - W(s)$ and $W(v) - W(u)$ are independent.

In numerical simulations, the standard Wiener process is discretized with a timestep dt as

$$dW \sim \sqrt{dt}N(0, 1)\,.$$

The probability $\Pi_a(x_0)$ of the first passage being through $x = a$, given that the starting point is x_0, is found from the boundary value problem (see equation (5.2.186) of [31])

$$g(x_0)\Pi_a'(x_0) + \frac{D(x_0)}{2}\Pi_a''(x_0) = 0\,,$$

$$\Pi_a(a) = 1, \qquad \Pi_a(b) = 0\,.$$

This follows from the backward Kolmogorov or Fokker-Planck equation [31]. Letting

$$\psi(x) = \exp\left(\int_a^x \frac{2g(y)}{D(y)}dy\right)\,, \tag{27}$$

we obtain the error rate

$$\text{ER} = \Pi_a(x_0) = \frac{F_{x_0}^b}{F_a^b}\,, \tag{28}$$

where

$$F_{x_1}^{x_2} = \int_{x_1}^{x_2} \frac{dy}{\psi(y)}. \tag{29}$$

(Note that equations (5.2.189) and (5.2.190) of [31] are incorrect.) The probability that a correct decision is made is

$$1 - \mathrm{ER} = \frac{F_a^{x_0}}{F_a^b} \,. \tag{30}$$

The mean first passage time $T(x_0)$, where the starting point is x_0 and passage is through $x = a$ *or* $x = b$, is found from the boundary value problem (see equation (5.2.154) of [31])

$$g(x_0)T'(x_0) + \frac{D(x_0)}{2}T''(x_0) = -1 \,,$$

$$T(a) = T(b) = 0.$$

This also follows from the backward Kolmogorov or Fokker-Planck equation [31]. Letting

$$f(y) = \frac{2}{\psi(y)} \int_a^y \frac{\psi(s)}{D(s)} ds, \qquad G_{x_1}^{x_2} = \int_{x_1}^{x_2} f(y) dy \,, \tag{31}$$

the mean reaction time is (see equation (5.1.158) of [31]).

$$\mathrm{RT} = T(x_0) = \frac{F_a^{x_0} G_{x_0}^b - F_{x_0}^b G_a^{x_0}}{F_a^b} \,. \tag{32}$$

As in §2, we define the reward rate RR to be the probability of a correct response divided by the average time between responses. Allowing an imposed delay $D \geq 0$ between trials and an additional penalty delay $D_p \geq 0$ after incorrect responses,

$$\mathrm{RR} = \frac{1 - \mathrm{ER}}{\mathrm{RT} + D + D_p \mathrm{ER}} \,. \tag{33}$$

We will find it more convenient to consider 1/RR, which, using (28), (32), and (33), may be written as:

$$\frac{1}{\mathrm{RR}} = D + G_{x_0}^b + (D + D_p - G_a^{x_0}) \frac{F_{x_0}^b}{F_a^{x_0}} \,. \tag{34}$$

3.2 The constant drift-diffusion equation

As our first example, consider the constant drift-diffusion equation

$$dy = A\, dt + c\, dW \,, \; y(0) = y_0 \,, \tag{35}$$

with thresholds $a_y = -z, b_y = z$. Without loss of generality, we take $A > 0$. Letting $y = Ax$ and defining

$$\tilde{z} = \frac{z}{A} > 0, \qquad \tilde{a} = \left(\frac{A}{c}\right)^2 > 0, \tag{36}$$

equation (35) becomes

$$dx = dt + \frac{1}{\sqrt{\tilde{a}}} dW \tag{37}$$

with thresholds $a = -\tilde{z}, b = \tilde{z}$, and initial condition $x_0 = \frac{y_0}{A}$: a special case of (26) with $g(x) = 1, D(x) = \frac{1}{\tilde{a}}$.

3.2.1 Error rates, mean reaction times, and reward rates

From (27), (29) and (31) it is readily shown that

$$\psi(y) = e^{2\tilde{a}(y+\tilde{z})}, \qquad f(y) = 1 - e^{-2\tilde{a}(y+\tilde{z})} \,,$$

and

$$F_a^{x_0} = \frac{1}{2\tilde{a}}\left(1 - e^{-2(\tilde{z}+x_0)\tilde{a}}\right) \,, \qquad F_{x_0}^b = \frac{e^{-2\tilde{z}\tilde{a}}}{2\tilde{a}}\left(e^{-2x_0\tilde{a}} - e^{-2\tilde{z}\tilde{a}}\right), \qquad F_a^b = \frac{1}{2\tilde{a}}\left(1 - e^{-4\tilde{z}\tilde{a}}\right) \,,$$

$$G_a^{x_0} = \tilde{z} + x_0 + \frac{1}{2\tilde{a}}\left(e^{-2(\tilde{z}+x_0)\tilde{a}} - 1\right), \qquad G_{x_0}^b = \tilde{z} - x_0 + \frac{1}{2\tilde{a}}e^{-2\tilde{z}\tilde{a}}\left(e^{-2\tilde{z}\tilde{a}} - e^{-2x_0\tilde{a}}\right) \,.$$

Thus, via (28), (32) and (34) we have:

$$\mathrm{ER} = \frac{1}{1+e^{2\tilde{z}\tilde{a}}} - \left\{\frac{1 - e^{-2x_0\tilde{a}}}{e^{2\tilde{z}\tilde{a}} - e^{-2\tilde{z}\tilde{a}}}\right\}, \tag{38}$$

$$\mathrm{RT} = \tilde{z}\tanh(\tilde{z}\tilde{a}) + \left\{\frac{2\tilde{z}(1 - e^{-2x_0\tilde{a}})}{e^{2\tilde{z}\tilde{a}} - e^{-2\tilde{z}\tilde{a}}} - x_0\right\} \,, \tag{39}$$

$$\frac{1}{\mathrm{RR}} = \tilde{z} + D + (D + D_p - \tilde{z})e^{-2\tilde{z}\tilde{a}} + \left\{\frac{(1+e^{2\tilde{z}\tilde{a}})[(D + D_p - \tilde{z})(1 - e^{2x_0\tilde{a}}) + x_0 e^{2x_0\tilde{a}}(1 - e^{2\tilde{z}\tilde{a}})]}{e^{2\tilde{z}\tilde{a}}(e^{2(\tilde{z}+x_0)\tilde{a}} - 1)}\right\} \,. \tag{40}$$

Note, in particular, that the error rate (38) may be made as small as we wish for a given drift and noise variance, by picking the threshold $\tilde{z} \sim z$ sufficiently high.

These expressions allow biased initial data, as suggested by the unequal salience case of Section 2.3, cf. equations (24-25), but for the remainder of this section and throughout the next we shall assume equal salience and unbiased initial data $x_0 = 0$, in which case the expressions in braces in (38-40) vanish identically.

Remark: We note that the expressions (38-39) agree with the analogous expressions for the discrete SPRT given in Section 2. Specifically, for unbiased initial data and equal error rates $\alpha_0 = \alpha_1 = \epsilon$, the scaled threshold definition of (25) may be rearranged to give

$$\epsilon = \frac{1}{1 + \exp\left(\frac{2Az}{c^2}\right)} = \frac{1}{1+e^{2\tilde{z}\tilde{a}}} \,,$$

and (7-8) reduce to

$$\left[(1-2\epsilon)\log\left(\frac{1-\epsilon}{\epsilon}\right)\right] \Big/ \left(\frac{2A^2}{c^2}\right) = \tilde{z}\tanh(\tilde{z}\tilde{a}) \,.$$

3.2.2 Optimizing reward rates for unbiased data

Suppose that we want to know the critical value of $\tilde{z}$, say $\tilde{z}_c$, which maximizes the reward rate RR, or, equivalently, which minimizes 1/RR. Setting $\frac{\partial}{\partial \tilde{z}}\left(\frac{1}{\mathrm{RR}}\right)\big|_{\tilde{z}=\tilde{z}_c} = 0$, $\tilde{z}_c$ is found from

$$e^{2\tilde{z}_c\tilde{a}} - 1 = 2\tilde{a}(D + D_p - \tilde{z}_c) \,. \tag{41}$$

The LHS of (41) vanishes at $\tilde{z}_c = 0$ and is monotonically increasing in $\tilde{z}_c$, while the RHS is positive at $\tilde{z}_c = 0$ (provided D and/or D_p is nonnegative) and is monotonically decreasing in $\tilde{z}_c$. There is thus a *unique* solution to (41). Moreover, it is a minimum because, using (41) to eliminate $(D + D_p)$, we have

$$\frac{\partial^2}{\partial \tilde{z}^2}\left(\frac{1}{\mathrm{RR}}\right)\bigg|_{\tilde{z}=\tilde{z}_c} = 2\tilde{a}e^{-2\tilde{z}_c\tilde{a}}[1 + e^{2\tilde{z}_c\tilde{a}}] > 0\,. \tag{42}$$

Thus, reward rate is maximized with respect to $\tilde{z}$ at $\tilde{z} = \tilde{z}_c(\tilde{a}, D, D_p)$. We note that since the LHS of (41) is greater than $2\tilde{z}_c\tilde{a}$, it is necessary that $\tilde{z}_c < (D + D_p)/2$.

Finally, it is useful to give limiting expressions for (40) for small and large $\tilde{z}$. Taylor expanding (40) in $\tilde{z}$ about $\tilde{z} = 0$, we find that for small $\tilde{z}$,

$$\frac{1}{\mathrm{RR}} \approx 2D + D_p - 2\tilde{a}(D + D_p)\tilde{z}. \tag{43}$$

On the other hand, using

$$\lim_{\alpha\to\infty} \alpha^n e^{-\alpha\tilde{a}} = 0 \tag{44}$$

for any integer $n \geq 0$ we find that for large $\tilde{z}$

$$\frac{1}{\mathrm{RR}} \approx D + \tilde{z}. \tag{45}$$

Figure 1 shows a plot of $1/\mathrm{RR}$ as a function of $\tilde{z}$, including the small and large $\tilde{z}$ approximations, for the parameters

$$\tilde{a} = 1, \qquad D = 10, \qquad D_p = 20.$$

Note that for these parameters, it is numerically determined that

$$\tilde{z}_c = 2.02115, \qquad \frac{1}{\mathrm{RR}}\bigg|_{\tilde{z}_c} = 12.5124, \qquad \mathrm{RR}|_{\tilde{z}_c} = 0.0799.$$

Remark: The error rate and reaction time expressions of (38-39), along with the condition for maximization of reward rate (41), permit us to derive a relationship among these two experimentally-measurable quantities and the inter-trial and penalty delays D and D_p, imposed by the experimenter. Specifically, for the unbiased ($x_0 = 0$) case, from (38) we have

$$e^{2\tilde{z}\tilde{a}} = \frac{1 - \mathrm{ER}}{\mathrm{ER}}\,,$$

and rewriting (39) as

$$\tilde{z} = \mathrm{RT}\left(\frac{e^{2\tilde{z}\tilde{a}} - 1}{e^{2\tilde{z}\tilde{a}} + 1}\right) = \frac{\mathrm{RT}}{1 - 2\mathrm{ER}}\,,$$

we may solve for $\tilde{z}$ and $\tilde{a}$ in terms of RT and ER to obtain:

$$\tilde{z} = \frac{\mathrm{RT}}{1 - 2\mathrm{ER}}\,, \; \tilde{a} = \frac{1 - 2\mathrm{ER}}{2\mathrm{RT}} \log\left(\frac{1 - \mathrm{ER}}{\mathrm{ER}}\right)\,. \tag{46}$$

In case of optimality, $\tilde{z}$ is given by (41), which, using (46), can be rewritten as:

$$D + D_p = \tilde{z}\left(1 + \frac{e^{2\tilde{z}\tilde{a}} - 1}{2\tilde{z}\tilde{a}}\right) = \mathrm{RT}\left(\frac{1}{1 - 2\mathrm{ER}} + \frac{1}{\mathrm{ER}\log\left[\frac{1-\mathrm{ER}}{\mathrm{ER}}\right]}\right). \tag{47}$$

Then, for error rates meaured under different imposed delays, one can compare subjects' actual mean reaction times with the optimal ones predicted by (47).

In the drift-diffusion model, the reaction time represents only the time taken to render a decision, e.g. the duration of neural integration until the firing rate reaches threshold [7]. In behavioral experiments, the *measured* reaction time includes additional 'fixed' durations required for visual processing and initiation of motor commands, which must typically be fitted as an additive constant (T_f). This requires modifying (47) to obtain:

$$[\text{behavioral response time}] - T_f = (D + D_p + T_f)\left(\frac{1}{1 - 2\mathrm{ER}} + \frac{1}{\mathrm{ER}\log\left[\frac{1-\mathrm{ER}}{\mathrm{ER}}\right]}\right)^{-1}; \tag{48}$$

see [1] for details.

3.3 The Ornstein-Uhlenbeck process

As our second example, consider the Ornstein-Uhlenbeck process

$$dy = (\lambda y + A)\,dt + c\,dW\,, \tag{49}$$

with thresholds $a_y = -z$, $b_y = z$. Letting

$$y = -\frac{A}{\lambda} + Ax$$

and using $\tilde{z}, \tilde{a}$ as defined in (36),

$$dx = \lambda x\,dt + \frac{1}{\sqrt{\tilde{a}}}\,dW\,, \tag{50}$$

with thresholds $a = -\tilde{z} + 1/\lambda$, $b = \tilde{z} + 1/\lambda$; that is, equation (26) with $g(x) = \lambda x$, $D(x) = 1/\tilde{a}$.

3.3.1 Error rates, mean reaction times, and reward rates

Suppose we have an unbiased initial condition, i.e., $y_0 = 0 \Rightarrow x_0 = 1/\lambda$. Then

$$\psi(y) = e^{\lambda\tilde{a}(y^2 - (\tilde{z} - 1/\lambda)^2)}, \qquad f(y) = 2\tilde{a}e^{-\lambda\tilde{a}y^2}\int_{-\tilde{z}+1/\lambda}^{y} e^{\lambda\tilde{a}s^2}ds,$$

giving

$$
\begin{aligned}
F_a^{x_0} &= \frac{1}{2}\sqrt{\frac{\pi}{\tilde{a}\lambda}}e^{\lambda\tilde{a}(-\tilde{z}+1/\lambda)^2}\left[\operatorname{erf}\left(\sqrt{\frac{\tilde{a}}{\lambda}}\right)-\operatorname{erf}\left(\sqrt{\frac{\tilde{a}}{\lambda}}(1-\lambda\tilde{z})\right)\right],\\
F_{x_0}^b &= \frac{1}{2}\sqrt{\frac{\pi}{\tilde{a}\lambda}}e^{\lambda\tilde{a}(-\tilde{z}+1/\lambda)^2}\left[\operatorname{erf}\left(\sqrt{\frac{\tilde{a}}{\lambda}}(1+\lambda\tilde{z})\right)-\operatorname{erf}\left(\sqrt{\frac{\tilde{a}}{\lambda}}\right)\right],\\
F_a^b &= \frac{1}{2}\sqrt{\frac{\pi}{\tilde{a}\lambda}}e^{\lambda\tilde{a}(-\tilde{z}+1/\lambda)^2}\left[\operatorname{erf}\left(\sqrt{\frac{\tilde{a}}{\lambda}}(1+\lambda\tilde{z})\right)-\operatorname{erf}\left(\sqrt{\frac{\tilde{a}}{\lambda}}(1-\lambda\tilde{z})\right)\right],\\
G_a^{x_0} &= \frac{2}{\lambda}\left\{\int_{\sqrt{\frac{\tilde{a}}{\lambda}}(1-\lambda\tilde{z})}^{\sqrt{\frac{\tilde{a}}{\lambda}}}\mathcal{D}(z)dz+\frac{\sqrt{\pi}}{2}K\left[\operatorname{erf}\left(\sqrt{\frac{\tilde{a}}{\lambda}}(1-\lambda\tilde{z})\right)-\operatorname{erf}\left(\sqrt{\frac{\tilde{a}}{\lambda}}\right)\right]\right\},\\
G_{x_0}^b &= \frac{2}{\lambda}\left\{\int_{\sqrt{\frac{\tilde{a}}{\lambda}}}^{\sqrt{\frac{\tilde{a}}{\lambda}}(1+\lambda\tilde{z})}\mathcal{D}(z)dz+\frac{\sqrt{\pi}}{2}K\left[\operatorname{erf}\left(\sqrt{\frac{\tilde{a}}{\lambda}}\right)-\operatorname{erf}\left(\sqrt{\frac{\tilde{a}}{\lambda}}(1+\lambda\tilde{z})\right)\right]\right\}.
\end{aligned}
$$

Here $\operatorname{erf}(z)=\frac{2}{\sqrt{\pi}}\int_0^z e^{-t^2}dt$ denotes the error function, $\operatorname{erfc}(z)=\frac{2}{\sqrt{\pi}}\int_z^\infty e^{-t^2}dt=1-\operatorname{erf}(z)$ is the complementary error function (used below),

$$
\mathcal{D}(z)=e^{-z^2}\int_0^z e^{t^2}dt \tag{51}
$$

is known as Dawson's integral, and we write

$$
K=\int_0^{\sqrt{\frac{\tilde{a}}{\lambda}}(1-\lambda\tilde{z})}e^{t^2}dt.
$$

Note that these formulae apply to both positive and negative λ, via the definition of the error function with imaginary argument: $\frac{2}{\sqrt{\pi}}\int_0^z e^{t^2}dt=\operatorname{erfi}(z)=i\operatorname{erf}(-iz)$.

Using the above expressions in (28), (32), and (33), we obtain

$$
\mathrm{ER}=\frac{\operatorname{erf}\left(\sqrt{\frac{\tilde{a}}{\lambda}}(1+\lambda\tilde{z})\right)-\operatorname{erf}\left(\sqrt{\frac{\tilde{a}}{\lambda}}\right)}{\operatorname{erf}\left(\sqrt{\frac{\tilde{a}}{\lambda}}(1+\lambda\tilde{z})\right)-\operatorname{erf}\left(\sqrt{\frac{\tilde{a}}{\lambda}}(1-\lambda\tilde{z})\right)}\stackrel{\text{def}}{=}\frac{\frac{\operatorname{erfc}(\cdot)}{\operatorname{erfc}(+)}-1}{\frac{\operatorname{erfc}(-)}{\operatorname{erfc}(+)}-1}, \tag{52}
$$

$$\begin{aligned}
\mathrm{RT} &= \frac{2}{\lambda\left[\mathrm{erf}\left(\sqrt{\frac{\tilde{a}}{\lambda}}(1+\lambda\tilde{z})\right)-\mathrm{erf}\left(\sqrt{\frac{\tilde{a}}{\lambda}}(1-\lambda\tilde{z})\right)\right]}\times \\
&\quad \left\{\left[\mathrm{erf}\left(\sqrt{\frac{\tilde{a}}{\lambda}}\right)-\mathrm{erf}\left(\sqrt{\frac{\tilde{a}}{\lambda}}(1-\lambda\tilde{z})\right)\right]\int_{\sqrt{\frac{\tilde{a}}{\lambda}}}^{\sqrt{\frac{\tilde{a}}{\lambda}}(1+\lambda\tilde{z})}\mathcal{D}(z)dz\right. \\
&\quad \left.+\left[\mathrm{erf}\left(\sqrt{\frac{\tilde{a}}{\lambda}}\right)-\mathrm{erf}\left(\sqrt{\frac{\tilde{a}}{\lambda}}(1+\lambda\tilde{z})\right)\right]\int_{\sqrt{\frac{\tilde{a}}{\lambda}}(1-\lambda\tilde{z})}^{\sqrt{\frac{\tilde{a}}{\lambda}}}\mathcal{D}(z)dz\right\} \\
&= \frac{2}{\lambda}\left\{\frac{\left[\frac{\mathrm{erfc}(-)}{\mathrm{erfc}(+)}-\frac{\mathrm{erfc}(\cdot)}{\mathrm{erfc}(+)}\right]\mathcal{D}_1-\left[\frac{\mathrm{erfc}(\cdot)}{\mathrm{erfc}(+)}-1\right]\mathcal{D}_2}{\frac{\mathrm{erfc}(-)}{\mathrm{erfc}(+)}-1}\right\},
\end{aligned} \tag{53}$$

$$\begin{aligned}
\frac{1}{\mathrm{RR}} &= D+\frac{2}{\lambda}\mathcal{D}_1+(D+D_p-\frac{2}{\lambda}\mathcal{D}_2)\left(\frac{\mathrm{erf}\left(\sqrt{\frac{\tilde{a}}{\lambda}}(1+\lambda\tilde{z})\right)-\mathrm{erf}\left(\sqrt{\frac{\tilde{a}}{\lambda}}\right)}{\mathrm{erf}\left(\sqrt{\frac{\tilde{a}}{\lambda}}\right)-\mathrm{erf}\left(\sqrt{\frac{\tilde{a}}{\lambda}}(1-\lambda\tilde{z})\right)}\right) \\
&= D+\frac{2}{\lambda}\mathcal{D}_1+(D+D_p-\frac{2}{\lambda}\mathcal{D}_2)\left\{\frac{\frac{\mathrm{erfc}(\cdot)}{\mathrm{erfc}(+)}-1}{\frac{\mathrm{erfc}(-)}{\mathrm{erfc}(+)}-\frac{\mathrm{erfc}(\cdot)}{\mathrm{erfc}(+)}}\right\}.
\end{aligned} \tag{54}$$

Here

$$\mathrm{erfc}(\cdot)=\mathrm{erfc}\left(\sqrt{\frac{\tilde{a}}{\lambda}}\right),\qquad \mathrm{erfc}(+)=\mathrm{erfc}\left(\sqrt{\frac{\tilde{a}}{\lambda}}(1+\lambda\tilde{z})\right),\qquad \mathrm{erfc}(-)=\mathrm{erfc}\left(\sqrt{\frac{\tilde{a}}{\lambda}}(1-\lambda\tilde{z})\right),$$

$$\mathcal{D}_1=\int_{\sqrt{\frac{\tilde{a}}{\lambda}}}^{\sqrt{\frac{\tilde{a}}{\lambda}}(1+\lambda\tilde{z})}\mathcal{D}(z)dz,\qquad \mathcal{D}_2=\int_{\sqrt{\frac{\tilde{a}}{\lambda}}(1-\lambda\tilde{z})}^{\sqrt{\frac{\tilde{a}}{\lambda}}}\mathcal{D}(z)dz.$$

Note that, in contrast to the constant drift ($\lambda = 0$) case of (38), (52) implies that even as the threshold $\tilde{z} \sim z$ is taken to infinity, the error rate remains strictly positive. Indeed, we have:

$$\lim_{\tilde{z}\to\infty}\mathrm{ER}=\frac{1}{2}\left[1-\mathrm{erf}\left(\sqrt{\frac{\tilde{a}}{\lambda}}\right)\right], \tag{55}$$

which only approaches zero as $\lambda \to 0$. See Figure 2.

3.3.2 Asymptotics for small λ and small and large $\tilde{z}$

Equipped with the exact expressions (52-54), in principle we can numerically calculate ER, RT, and 1/RR for any values of the parameters $\tilde{z}, \tilde{a}, \lambda, D$, and D_p. However, the evaluation of the integrals in the formulas becomes difficult for small λ, which turns out to be the region of greatest interest. Also, it is difficult from the exact formulae to see how ER, RT, and 1/RR vary with the parameters. To gain insight into these issues, we now expand the expressions for small λ. Note that we treat $\tilde{z}$ as an $\mathcal{O}(1)$ quantity to obtain the following expansions.

First, we recall the expansion of the complementary error function for large z [33, equation (7.1.23)]:

$$\operatorname{erfc}(z) = \frac{e^{-z^2}}{\sqrt{\pi}z}\left(1 - \frac{1}{2z^2} + \frac{3}{4z^4} + \cdots\right).$$

This gives

$$\begin{aligned}\frac{\operatorname{erfc}(-)}{\operatorname{erfc}(+)} &= e^{4\tilde{z}\tilde{a}}\left(\frac{1+\lambda\tilde{z}}{1-\lambda\tilde{z}}\right)\frac{\left(1 - \frac{\lambda}{2\tilde{a}(1-\lambda\tilde{z})^2} + \frac{3\lambda^2}{4\tilde{a}^2(1-\lambda\tilde{z})^4} + \cdots\right)}{\left(1 - \frac{\lambda}{2\tilde{a}(1+\lambda\tilde{z})^2} + \frac{3\lambda^2}{4\tilde{a}^2(1+\lambda\tilde{z})^4} + \cdots\right)} \\ &= e^{4\tilde{z}\tilde{a}}\left(1 + 2\tilde{z}\lambda + \frac{2\tilde{z}(\tilde{z}\tilde{a}-1)}{\tilde{a}}\lambda^2\right) + \mathcal{O}(\lambda^3), \end{aligned} \tag{56}$$

$$\begin{aligned}\frac{\operatorname{erfc}(\cdot)}{\operatorname{erfc}(+)} &= e^{2\tilde{z}\tilde{a}+\tilde{z}^2\tilde{a}\lambda}(1+\lambda\tilde{z})\frac{\left(1 - \frac{\lambda}{2\tilde{a}} + \frac{3\lambda^2}{4\tilde{a}^2} + \cdots\right)}{\left(1 - \frac{\lambda}{2\tilde{a}(1+\lambda\tilde{z})^2} + \frac{3\lambda^2}{4\tilde{a}^2(1+\lambda\tilde{z})^4} + \cdots\right)} \\ &= e^{2\tilde{z}\tilde{a}}\left(1 + \tilde{z}(1+\tilde{z}\tilde{a})\lambda + \frac{\tilde{z}}{2\tilde{a}}(\tilde{z}^3\tilde{a}^3 + 2\tilde{z}^2\tilde{a}^2 - 2)\lambda^2\right) + \mathcal{O}(\lambda^3). \end{aligned} \tag{57}$$

We also use the following expansion for Dawson's integral from [34] equation (42.6.6), valid for large z:

$$\mathcal{D}(z) = \frac{1}{2z} + \frac{1}{4z^3} + \frac{3}{8z^5} + \cdots.$$

This implies that

$$\mathcal{D}_1 = \frac{\tilde{z}}{2}\lambda + \frac{\tilde{z}(1-\tilde{z}\tilde{a})}{4\tilde{a}}\lambda^2 + \frac{\tilde{z}(9(1-\tilde{z}\tilde{a}) + 4\tilde{z}^2\tilde{a}^2)}{24\tilde{a}^2}\lambda^3 + \mathcal{O}(\lambda^4), \tag{58}$$

$$\mathcal{D}_2 = \frac{\tilde{z}}{2}\lambda + \frac{\tilde{z}(1+\tilde{z}\tilde{a})}{4\tilde{a}}\lambda^2 + \frac{\tilde{z}(9(1+\tilde{z}\tilde{a}) + 4\tilde{z}^2\tilde{a}^2)}{24\tilde{a}^2}\lambda^3 + \mathcal{O}(\lambda^4). \tag{59}$$

Using these formulas in (52), (53), and (54) gives the approximations

$$\mathrm{ER} = \mathrm{ER}_0 + \lambda\mathrm{ER}_1 + \lambda^2\mathrm{ER}_2 + \mathcal{O}(\lambda^3), \tag{60}$$

where

$$\mathrm{ER}_0 = \frac{1}{1+e^{2\tilde{z}\tilde{a}}},$$

$$\mathrm{ER}_1 = \frac{\tilde{z}e^{2\tilde{z}\tilde{a}}}{e^{4\tilde{z}\tilde{a}}-1}(\tilde{z}\tilde{a} - \tanh(\tilde{z}\tilde{a})),$$

$$\begin{aligned}\mathrm{ER}_2 = {} & \tilde{z}e^{2\tilde{z}\tilde{a}}(-4\tilde{z}\tilde{a}e^{2\tilde{z}\tilde{a}}(-1+e^{2\tilde{z}\tilde{a}}) + 2(-1+e^{2\tilde{z}\tilde{a}})^2(1+e^{2\tilde{z}\tilde{a}}) + \tilde{z}^3\tilde{a}^3(-1+e^{2\tilde{z}\tilde{a}})(1+e^{2\tilde{z}\tilde{a}})^2 \\ & -2\tilde{z}^2\tilde{a}^2(1+e^{2\tilde{z}\tilde{a}}+e^{4\tilde{z}\tilde{a}}+e^{6\tilde{z}\tilde{a}}))/(2\tilde{a}(-1+e^{2\tilde{z}\tilde{a}})^2(1+e^{2\tilde{z}\tilde{a}})^3),\end{aligned}$$

$$\mathrm{RT} = \mathrm{RT}_0 + \lambda\mathrm{RT}_1 + \lambda^2\mathrm{RT}_2 + \mathcal{O}(\lambda^3), \tag{61}$$

where

$$\mathrm{RT}_0 = \tilde{z}\tanh(\tilde{z}\tilde{a}),$$

$$\text{RT}_1 = \tilde{z}\left\{\frac{\tanh(\tilde{z}\tilde{a}) - \tilde{z}\tilde{a}}{2\tilde{a}} + \frac{2\tilde{z}e^{2\tilde{z}\tilde{a}}}{e^{4\tilde{z}\tilde{a}}-1}[e^{2\tilde{z}\tilde{a}}(1-\tanh(\tilde{z}\tilde{a})) - (1+\tilde{z}\tilde{a})]\right\},$$

$$\begin{aligned}\text{RT}_2 \;=\; & \tilde{z}(-12\tilde{z}^4\tilde{a}^4e^{2\tilde{z}\tilde{a}}(-1+e^{2\tilde{z}\tilde{a}})(1+e^{2\tilde{z}\tilde{a}})^2 + 9(-1+e^{2\tilde{z}\tilde{a}})^3(1+e^{2\tilde{z}\tilde{a}})^2 \\ & +4\tilde{z}^2\tilde{a}^2(-1+e^{2\tilde{z}\tilde{a}})^3(1-e^{2\tilde{z}\tilde{a}}+e^{4\tilde{z}\tilde{a}}) + 24\tilde{z}^3\tilde{a}^3e^{2\tilde{z}\tilde{a}}(1+e^{2\tilde{z}\tilde{a}}+e^{4\tilde{z}\tilde{a}}+e^{6\tilde{z}\tilde{a}}) \\ & -3\tilde{z}\tilde{a}(-1+e^{2\tilde{z}\tilde{a}})^2(3+13e^{2\tilde{z}\tilde{a}}+13e^{4\tilde{z}\tilde{a}}+3e^{6\tilde{z}\tilde{a}}))/(12\tilde{a}^2(-1+e^{2\tilde{z}\tilde{a}})^2(1+e^{2\tilde{z}\tilde{a}})^3),\end{aligned}$$

$$\frac{1}{\text{RR}} = A_0 + \lambda A_1 + \lambda^2 A_2 + \mathcal{O}(\lambda^3), \tag{62}$$

where

$$A_0 = \tilde{z} + D + (D + D_p - \tilde{z})e^{-2\tilde{z}\tilde{a}},$$

$$A_1 = \tilde{z}\left[\frac{(1-\tilde{z}\tilde{a})(1-e^{-2\tilde{z}\tilde{a}})}{2\tilde{a}} - (D+D_p)e^{-2\tilde{z}\tilde{a}} + (D+D_p-\tilde{z})\tilde{z}\tilde{a}e^{-2\tilde{z}\tilde{a}}\left(\frac{e^{2\tilde{z}\tilde{a}}+1}{e^{2\tilde{z}\tilde{a}}-1}\right)\right],$$

$$\begin{aligned}A_2 \;=\; & \tilde{z}(-6\tilde{z}^4\tilde{a}^4(1+e^{2\tilde{z}\tilde{a}})^2 - 3\tilde{z}\tilde{a}(-1+e^{2\tilde{z}\tilde{a}})(-5+2e^{2\tilde{z}\tilde{a}}+3e^{4\tilde{z}\tilde{a}}+4\tilde{a}(D+D_p)) \\ & +3(-1+e^{2\tilde{z}\tilde{a}})^2(3(-1+e^{2\tilde{z}\tilde{a}})+4\tilde{a}(D+D_p)) \\ & +6\tilde{z}^3\tilde{a}^3(-1+4e^{2\tilde{z}\tilde{a}}+e^{4\tilde{z}\tilde{a}}+\tilde{a}(1+e^{2\tilde{z}\tilde{a}})^2(D+D_p)) \\ & -4\tilde{z}^2\tilde{a}^2(-(-1+e^{2\tilde{z}\tilde{a}})^3+3\tilde{a}(-1+2e^{2\tilde{z}\tilde{a}}+e^{4\tilde{z}\tilde{a}})(D+D_p)))/(12\tilde{a}^2e^{2\tilde{z}\tilde{a}}(-1+e^{2\tilde{z}\tilde{a}})^2).\end{aligned}$$

Here the $\mathcal{O}(\lambda^2)$ expressions were obtained using Mathematica. Notice that for $\lambda = 0$, equations (60), (61), and (62) are identical to equations (38), (39), and (40). We verify the validity of these approximations in Figures 3, 4, and 5.

It is also instructive to find approximations for 1/RR for small and large $\tilde{z}$; to obtain these, we start with the expression for 1/RR valid to $\mathcal{O}(\lambda^2)$, then consider the limit in $\tilde{z}$. Using an analogue to (44), we find that for small $\tilde{z}$

$$\frac{1}{\text{RR}} \approx 2D + D_p - 2\tilde{a}(D+D_p)\tilde{z}, \tag{63}$$

as for the constant drift-diffusion equation (cf. (43)). For large $\tilde{z}$,

$$\begin{aligned}\frac{1}{\text{RR}} \;&\approx\; D + \tilde{z} + \lambda\frac{\tilde{z}}{2}\left(\frac{1}{\tilde{a}} - \tilde{z}\right) + \lambda^2\tilde{z}\left(\frac{9(1-\tilde{z}\tilde{a}) + 4\tilde{z}^2\tilde{a}^2}{12\tilde{a}^2}\right) \\ &\to\; \frac{\lambda^2\tilde{z}^3}{3} \;\text{ for }\; \tilde{z}\to\infty. \quad (\lambda \neq 0)\end{aligned} \tag{64}$$

The validity of these results is examined in Figure 6.

3.3.3 Optimizing reward rates for unbiased data

We now show that $(\tilde{z}, \lambda) = (\tilde{z}_c, 0)$, where $\tilde{z}_c$ is found from (41), minimizes 1/RR, i.e., maximizes RR. First, using (41), we have

$$\frac{\partial}{\partial\tilde{z}}\left(\frac{1}{\text{RR}}\right)\bigg|_{(\tilde{z},\lambda)=(\tilde{z}_c,0)} = \frac{\partial A_0}{\partial\tilde{z}}\bigg|_{\tilde{z}=\tilde{z}_c} = 0. \tag{65}$$

Now, from (62),

$$\begin{aligned}\frac{\partial}{\partial\lambda}\left(\frac{1}{\mathrm{RR}}\right)\bigg|_{(\tilde{z},\lambda)=(\tilde{z}_c,0)} &= A_1|_{\tilde{z}=\tilde{z}_c} \\ &= \tilde{z}_c e^{-2\tilde{z}_c\tilde{a}}\left[\frac{(1-\tilde{z}_c\tilde{a})(e^{2\tilde{z}_c\tilde{a}}-1)}{2\tilde{a}} - (D+D_p) + (D+D_p-\tilde{z}_c)\tilde{z}_c\tilde{a}\left(\frac{e^{2\tilde{z}_c\tilde{a}}+1}{e^{2\tilde{z}_c\tilde{a}}-1}\right)\right].\end{aligned} \quad (66)$$

Solving (41) for $e^{2\tilde{z}_c\tilde{a}}$ and substituting into (66), we find that all terms cancel, i.e.,

$$\frac{\partial}{\partial\lambda}\left(\frac{1}{\mathrm{RR}}\right)\bigg|_{(\tilde{z},\lambda)=(\tilde{z}_c,0)} = 0. \quad (67)$$

The point $(\tilde{z},\lambda) = (\tilde{z}_c, 0)$ is called a *stationary point* because conditions (65) and (67) are satisfied.

The condition for the stationary point $(\tilde{z},\lambda) = (\tilde{z}_c, 0)$ to be a local optimum involves the Hessian of $1/\mathrm{RR}$ evaluated at the stationary point, i.e.,

$$H \equiv \begin{pmatrix} \frac{\partial^2}{\partial\lambda^2}\left(\frac{1}{\mathrm{RR}}\right)\Big|_{(\tilde{z},\lambda)=(\tilde{z}_c,0)} & \frac{\partial^2}{\partial\tilde{z}\partial\lambda}\left(\frac{1}{\mathrm{RR}}\right)\Big|_{(\tilde{z},\lambda)=(\tilde{z}_c,0)} \\ \frac{\partial^2}{\partial\tilde{z}\partial\lambda}\left(\frac{1}{\mathrm{RR}}\right)\Big|_{(\tilde{z},\lambda)=(\tilde{z}_c,0)} & \frac{\partial^2}{\partial\tilde{z}^2}\left(\frac{1}{\mathrm{RR}}\right)\Big|_{(\tilde{z},\lambda)=(\tilde{z}_c,0)} \end{pmatrix}. \quad (68)$$

The stationary point is a local minimizer (resp., maximizer) of $1/\mathrm{RR}$ if H is positive (resp., negative) definite, that is, if H has two positive (resp., two negative) eigenvalues. If H has one positive and one negative eigenvalue, then the stationary point is called a saddle point, and it is neither a local minimizer nor a local maximizer.

From (42),

$$\frac{\partial^2}{\partial\tilde{z}^2}\left(\frac{1}{\mathrm{RR}}\right)\bigg|_{(\tilde{z},\lambda)=(\tilde{z}_c,0)} = \frac{\partial^2 A_0}{\partial\tilde{z}^2}\bigg|_{\tilde{z}=\tilde{z}_c} = 2\tilde{a}e^{-2\tilde{z}_c\tilde{a}}[1+e^{2\tilde{z}_c\tilde{a}}] > 0. \quad (69)$$

Using this we conclude that if $\det(H) > 0$, then H is positive definite. Using (41) to eliminate $(D+D_p)$,

$$\begin{aligned}\frac{\partial^2}{\partial\lambda^2}\left(\frac{1}{\mathrm{RR}}\right)\bigg|_{(\tilde{z},\lambda)=(\tilde{z}_c,0)} &= 2A_2|_{\tilde{z}=\tilde{z}_c} \\ &= \frac{\tilde{z}_c[15(e^{2\tilde{z}_c\tilde{a}}-1)^2 - 9\tilde{z}_c\tilde{a}(e^{4\tilde{z}_c\tilde{a}}-1) + 3\tilde{z}_c^3\tilde{a}^3(e^{4\tilde{z}_c\tilde{a}}-1) - 2\tilde{z}_c^2\tilde{a}^2(1+10e^{2\tilde{z}_c\tilde{a}}+e^{4\tilde{z}_c\tilde{a}})]}{6\tilde{a}^2 e^{2\tilde{z}_c\tilde{a}}(e^{2\tilde{z}_c\tilde{a}}-1)},\end{aligned}$$

$$\begin{aligned}\frac{\partial^2}{\partial\tilde{z}\partial\lambda}\left(\frac{1}{\mathrm{RR}}\right)\bigg|_{(\tilde{z},\lambda)=(\tilde{z}_c,0)} &= \frac{\partial A_1}{\partial\tilde{z}}\bigg|_{\tilde{z}=\tilde{z}_c} \\ &= \frac{\tilde{z}_c(1+e^{2\tilde{z}_c\tilde{a}})(1-e^{2\tilde{z}_c\tilde{a}}+\tilde{z}_c\tilde{a}(1+e^{2\tilde{z}_c\tilde{a}}))}{e^{2\tilde{z}_c\tilde{a}}(1-e^{2\tilde{z}_c\tilde{a}})}.\end{aligned}$$

From these expressions, after simplifying, the condition that $\det(H) > 0$ becomes

$$\begin{aligned}0 < \det(H) &= \tilde{z}_c(1+e^{2\tilde{z}_c\tilde{a}})(15(e^{2\tilde{z}_c\tilde{a}}-1)^3 + 4\tilde{z}_c^2\tilde{a}^2(e^{2\tilde{z}_c\tilde{a}}-1)^3 - 12\tilde{z}_c^3\tilde{a}^3 e^{2\tilde{z}_c\tilde{a}}(1+e^{2\tilde{z}_c\tilde{a}}) \\ &\quad -12\tilde{z}_c\tilde{a}(e^{2\tilde{z}_c\tilde{a}}-1)^2(1+e^{2\tilde{z}_c\tilde{a}}))/(3\tilde{a}e^{4\tilde{z}_c\tilde{a}}(e^{2\tilde{z}_c\tilde{a}}-1)^2).\end{aligned} \quad (70)$$

For example, for

$$\tilde{a} = 1, \qquad D = 10, \qquad D_p = 20,$$

recalling that $\tilde{z}_c = 2.02115$, we find that

$$H = \begin{pmatrix} 3.9253 & -2.2487 \\ -2.2487 & 2.0351 \end{pmatrix}, \qquad \det(H) = 2.9317 > 0;$$

thus, $(\tilde{z}, \lambda) = (\tilde{z}_c, 0)$ is a local minimizer of $1/\text{RR}$, that is, a local maximizer of RR. For reference, the eigenvalues of H for these parameters are 5.4194 and 0.5410. Although we have not been able to prove that $\det(H)$ is positive for all possible parameter values, it is found numerically to be true for all choices considered: see Table 1. We can interpret these results as follows: given λ, it is possible to choose $\tilde{z}_c(\lambda)$ (say, by choosing the threshold z) to maximize the reward rate RR; however, it is even better to first adjust so that $\lambda = 0$, *then* choose $\tilde{z}$ to maximize RR. This is illustrated in Figure 7, which also emphasizes that care must be used in applying the $\mathcal{O}(\lambda)$ formulas.

We note that, even though the parameters in the Ornstein-Uhlenbeck first passage problem may be reduced to three: $\tilde{z}, \tilde{a}$ and λ (or two, if we take $\lambda = 0$ at its optimal value), it is still of interest to see how the threshold z_c that maximizes RR depends upon the original drift and noise r.m.s. parameters A, c, and on the delay parameters D, D_p. Figure 8 illustrates these dependences, and also shows the approximations valid for small and large values of the parameters:

$$\begin{aligned} z_c &\approx \frac{A}{2}(D + D_p)\,, \quad \text{for large } c, \text{ or small } D + D_p, \text{ or small } A, \\ z_c &\approx \frac{c^2}{2A} \log\left[\frac{2A^2}{c^2}(D + D_p)\right]\,, \quad \text{for small } c, \text{ or large } D + D_p, \text{ or large } A. \end{aligned}$$

3.4 Biased decisions

As discussed at the end of Section 2, the SPRT allows for unequal prior stimulus probabilities by biasing the thresholds, or, equivalently, biasing the initial condition taken in the drift-diffusion process, cf. (24). We consider this only for the (optimal) constant drift process (35)-(37). As above, we denote the probability of stimuli $\mathcal{S}_1$ and $\mathcal{S}_0$ (drifts $\pm A$) as Π and $1 - \Pi$ respectively, and the error rates and mean reaction times as $\text{ER}(\pm)$, $\text{RT}(\pm)$. The net error rate and mean reaction time are then given by:

$$\text{NER} = \Pi\,\text{ER}(+) + (1 - \Pi)\,\text{ER}(-) \quad \text{and} \quad \text{NRT} = \Pi\,\text{RT}(+) + (1 - \Pi)\,\text{RT}(-)\,. \tag{71}$$

We note that error rates and reaction times for biased initial data, as given in (38-39), apply to the case $A > 0$, but that the reflection transformation $x \mapsto -x$ takes sample paths of (37) with $A > 0$ to those for $A < 0$; we may thus simply substitute $-x_0$ for x_0 in those expressions to obtain $\text{ER}(-)$ and $\text{RT}(-)$, which yields:

$$\text{NER} = \frac{1}{1 + e^{2\tilde{z}\tilde{a}}} - \left\{\frac{1 - \Pi e^{-2x_0\tilde{a}} - (1 - \Pi)e^{2x_0\tilde{a}}}{e^{2\tilde{z}\tilde{a}} - e^{-2\tilde{z}\tilde{a}}}\right\}, \tag{72}$$

$$\text{NRT} = \tilde{z}\tanh\tilde{z}\tilde{a} + 2\tilde{z}\left\{\frac{1 - \Pi e^{-2x_0\tilde{a}} - (1 - \Pi)e^{2x_0\tilde{a}}}{e^{2\tilde{z}\tilde{a}} - e^{-2\tilde{z}\tilde{a}}}\right\} + (1 - 2\Pi)x_0\,. \tag{73}$$

Table 1: Critical value $\tilde{z}_c$ from (41) and $\det(H)$ from (70) for various choices of $\tilde{a}$ and $D + D_p$.

$\tilde{a}$	$D + D_p$	$\tilde{z}_c$	$\det(H)$
0.1	0.1	0.0498754	9.48718×10^{-13}
0.1	1	0.487711	7.60411×10^{-7}
0.1	3	1.39326	0.000347637
0.1	10	3.9603	0.116954
0.1	30	8.36411	5.41652
0.1	100	14.4806	70.2726
1	0.1	0.0487712	7.6042×10^{-9}
1	1	0.39603	0.00116954
1	3	0.836411	0.0541652
1	10	1.44806	0.702726
1	30	2.02115	2.93172
1	100	2.63835	8.53829
3	0.1	0.046442	3.86264×10^{-7}
3	1	0.278804	0.00601835
3	3	0.464314	0.0656822
3	10	0.673718	0.325746
3	30	0.861587	0.875563
3	100	1.06465	1.97395
10	0.1	0.039603	1.16954×10^{-5}
10	1	0.144806	0.00702726
10	3	0.202115	0.0293172
10	10	0.263835	0.0853829
10	30	0.319395	0.177656
10	100	0.37988	0.338872
30	0.1	0.0278804	6.01835×10^{-5}
30	1	0.0673718	0.00325746
30	3	0.0861587	0.00875563
30	10	0.106465	0.0197395
30	30	0.124865	0.0357598
30	100	0.144971	0.061673
100	0.1	0.0144806	7.02726×10^{-5}
100	1	0.0263835	0.000853829
100	3	0.0319395	0.00177656
100	10	0.037988	0.00338872
100	30	0.0434912	0.00555057
100	100	0.0495152	0.00884229

Use of the appropriate (optimal) biased initial condition (24), which may be written in the following form in the scaled variables

$$x_0 = \frac{y_0}{A} = \frac{1}{2\tilde{a}} \log\left(\frac{\Pi}{1-\Pi}\right) \Leftrightarrow e^{2x_0\tilde{a}} = \frac{\Pi}{1-\Pi}\,, \tag{74}$$

then gives the final expressions:

$$\text{NER} \equiv \frac{1}{1+e^{2\tilde{z}\tilde{a}}}\,, \tag{75}$$

$$\text{NRT} = \tilde{z}\tanh\tilde{z}\tilde{a} + \frac{(1-2\Pi)}{2\tilde{a}} \log\left(\frac{\Pi}{1-\Pi}\right)\,. \tag{76}$$

It is interesting to note that, for fixed $\tilde{z}$ and $\tilde{a}$, the ER takes the same value for *all* $0 \leq \Pi \leq 1$ and that DTs decrease symmetrically from the maximum at $\Pi = 1/2$ to zero at $\Pi = 1/(1+e^{\pm 2\tilde{z}\tilde{a}})$, for which values the initial condition falls on a threshold. Moreover, the biased initial condition (74) also maximizes the reward rate. Modifying the definition of (33) to read

$$\text{NRR} = \frac{1-\text{NER}}{\text{NDT}+D+T_0+D_p\text{NER}}\,, \tag{77}$$

a lengthy calculation reveals that

$$\frac{\partial}{\partial\tilde{z}}(\text{NRR}) = \frac{\partial}{\partial x_0}(\text{NRR}) = 0 \tag{78}$$

with x_0 given by (74) and $\tilde{z}$ by the solution $\tilde{z}_o$ of

$$e^{2\tilde{z}_o\tilde{a}} - 1 = 2\tilde{a}(D+D_p-\tilde{z}_o) + (1-2\Pi) \log\left(\frac{\Pi}{1-\Pi}\right)\,. \tag{79}$$

We have checked (numerically) that this critical point is indeed a maximum. Hence, noting that the final term in (79) is even about $\Pi = 1/2$ and strictly negative for $\Pi \neq 1/2$, this formula shows explicitly how optimal thresholds are lowered in choice tasks with stimuli of unequal salience. Moreover, we may compute a relationship among the salience Π, the total delay $D + D_p$ and the signal-to-noise ratio $\tilde{a}$ at which the optimal bias and optimal threshold coincide. Setting $x_o = \tilde{z}_o$ and replacing them in (79) by means of (74), we obtain:

$$\tilde{a} = \frac{\left[\frac{2\Pi-1}{1-\Pi} + 2\Pi\log\left(\frac{\Pi}{1-\Pi}\right)\right]}{2(D+D_p)}\,. \tag{80}$$

Note that, as expected, (80) gives $\tilde{a} = 0$ for $\Pi = 1/2$, and $\tilde{a}$ increases as Π increases from 1/2 or $D + D_p$ decreases with $\Pi \neq 1/2$. For $\tilde{a}$ less than the value given by (80), $x_o > \tilde{z}_o$, which implies that the more salient stimulus should be selected immediately upon presentation.

3.5 More on optimal thresholds

3.5.1 Dependence of the optimal threshold on experimental delays

In this Section we show that the dependence of the optimal threshold on $D+D_p$ (rather than D and D_p separately) is true for any decision maker. Consider a decision maker whose error rate

ER(z) and reaction time RT(z) are functions of the decision threshold z. As for the previous decision models, for the optimal threshold the derivative of 1/RR must be equal to zero. Using elementary calculations we compute the derivative:

$$\frac{\partial}{\partial z}\left(\frac{1}{\mathrm{RR}}\right) = \frac{\mathrm{RT}'(z) + \mathrm{ER}'(z)\,(D + D_p) - \mathrm{RT}'(z)\mathrm{ER}(z) + \mathrm{RT}(z)\mathrm{ER}'(z)}{(1 - \mathrm{ER}(z))^2}$$

Note that the above derivative does not depend on D and D_p separately, but only depends on $D + D_p$. Therefore the optimal threshold must also depend only on $D + D_p$ for any decision maker.

3.5.2 Reward rates with uncertain thresholds

In this subsection we consider the case in which a small error of ε is made in estimation of the optimal threshold $\tilde{z}_o$. We show that overestimation of the threshold results in higher reward rate than underestimation of the threshold, i.e.:

$$\mathrm{RR}(\tilde{z}_o + \varepsilon) - \mathrm{RR}(\tilde{z}_o - \varepsilon) > 0. \tag{81}$$

The implication is that, if the threshold cannot be set precisely, the best alternative is to set it slightly too high (on average). Behavioral data presented in [1] is consistent with this prediction, presumably due to adaptive learning strategies employed by task participants.

From Taylor expansion we obtain:

$$\mathrm{RR}(\tilde{z}_o + \varepsilon) = \mathrm{RR}(\tilde{z}_o) + \mathrm{RR}'(\tilde{z}_o)\varepsilon + \frac{\mathrm{RR}''(\tilde{z}_o)}{2}\varepsilon^2 + \frac{\mathrm{RR}'''(\tilde{z}_o)}{6}\varepsilon^3 + \mathcal{O}(4) + \mathcal{O}(5),$$

$$\mathrm{RR}(\tilde{z}_o - \varepsilon) = \mathrm{RR}(\tilde{z}_o) - \mathrm{RR}'(\tilde{z}_o)\varepsilon + \frac{\mathrm{RR}''(\tilde{z}_o)}{2}\varepsilon^2 - \frac{\mathrm{RR}'''(\tilde{z}_o)}{6}\varepsilon^3 + \mathcal{O}(4) - \mathcal{O}(5).$$

Since $\tilde{z}_o$ is the threshold maximizing RR, thus $\mathrm{RR}'(\tilde{z}_o) = 0$, and hence

$$\mathrm{RR}(\tilde{z}_o + \varepsilon) - \mathrm{RR}(\tilde{z}_o - \varepsilon) = \frac{\mathrm{RR}'''(\tilde{z}_o)}{3}\varepsilon^3 + \mathcal{O}(5).$$

To prove (81), it therefore suffices to show that $\mathrm{RR}'''(\tilde{z}_o) > 0$. In the beginning of this section we noticed that instead of considering RR, it is more convenient to consider its inverse 1/RR; let us denote it by $f = 1/\mathrm{RR}$. Using the chain rule and the fact that $f'(\tilde{z}_o) = 0$ we compute that:

$$\mathrm{RR}'''(\tilde{z}_o) = \frac{\partial^3}{\partial \tilde{z}^3}\left(\frac{1}{f(\tilde{z}_o)}\right) = -\frac{f'''(\tilde{z}_o)}{(f(\tilde{z}_o))^2}.$$

Since the denominator of the above equation is positive, for small ε inequality (81) is equivalent to $f'''(\tilde{z}_o) < 0$. Elementary calculations show that

$$f'''(\tilde{z}_o) = -4\tilde{a}^2 e^{-2\tilde{z}_o\tilde{a}}\left(3 + 2\tilde{a}(D + D_p - \tilde{z}_o)\right),$$

and substituting the condition for the optimal threshold (41) into this equation, we obtain

$$f'''(\tilde{z}_o) = -4\tilde{a}^2 e^{-2\tilde{z}_o\tilde{a}}\left(2 + e^{2\tilde{z}_o\tilde{a}}\right) < 0,$$

which yields (81).

4 Optimal Decisions under the Interrogation Protocol

We now suppose that subjects are interrogated at a fixed time after stimulus onset, and required to respond as soon as possible after interrogation. The appropriate model is again a drift-diffusion process, but now sample paths are assumed to evolve freely until interrogation, at which instant we interpret the probability of responses $\mathcal{R}_0$ and $\mathcal{R}_1$ by asking if a given sample path is closer to the threshold at $y = -z$ or the threshold at $y = +z$, respectively (cf., for example, [9]). This is the continuum analog of the Neyman-Pearson test. Specifically, we evaluate the integrals of the probability distribution of solutions of the forward Kolmogorov or Fokker-Planck equation between $-\infty$ and 0 and 0 and $+\infty$ respectively, to evaluate the expected %-correct and error rates. Note that, in this case a sample path may cross and recross either threshold multiple times, or cross neither, during the interval before interrogation.

4.1 General considerations

There are two common ways to interpret the stochastic differential equation (26). In the Itô (resp., Stratonovich) interpretation, stochastic integrals are approximated according to a "left-hand" (resp., "midpoint") sum [31, 32]. Taking the Itô interpretation, the probability distribution function $p(x,t)$ for solutions to (26) satisfies the forward Kolmogorov or Fokker-Planck equation (see (4.3.20) of [31], with corrected typo)

$$\frac{\partial p(x,t)}{\partial t} = -\frac{\partial}{\partial x}[g(x)p(x,t)] + \frac{1}{2}\frac{\partial^2}{\partial x^2}[D(x)p(x,t)]. \tag{82}$$

If, on the other hand, (26) is considered according to the Stratonovich interpretation, it may be shown to be equivalent to the Itô stochastic differential equation (see Eqn. (4.3.40) of [31])

$$dx = \left[g(x) + \frac{1}{2}\sqrt{D(x)}\frac{\partial\sqrt{D(x)}}{\partial x}\right] + \sqrt{D(x)}dW(t),$$

with associated forward Kolmogorov or Fokker-Planck equation (see (4.3.45) of [31])

$$\frac{\partial p(x,t)}{\partial t} = -\frac{\partial}{\partial x}[g(x)p(x,t)] + \frac{1}{2}\frac{\partial}{\partial x}\left[\sqrt{D(x)}\frac{\partial}{\partial x}[\sqrt{D(x)}p(x,t)]\right]. \tag{83}$$

In the following we consider cases where D is independent of x; then the Itô and Stratonovich interpretations give identical equations.

4.2 The Ornstein-Uhlenbeck process

We again consider the Ornstein-Uhlenbeck process of (49):

$$dy = (\lambda y + A)\,dt + c\,dW\,. \tag{84}$$

Including the limit $\lambda \to 0$, this encompasses both the cases treated above.

The forward Kolmogorov or Fokker-Planck equation governing the evolution of $p(y,t)dy$, the probability that a solution of (84) occupies a point in $[y, y+dy]$ at time t, is

$$\frac{\partial p}{\partial t} = -\frac{\partial}{\partial y}((\lambda y + A)p) + \frac{c^2}{2}\frac{\partial^2 p}{\partial y^2}\,; \qquad y \in (-\infty,\infty)\,,\ t \geq 0\,. \tag{85}$$

This initial-boundary value problem is solved by an evolving normal distribution:

$$p(y,t) = \frac{1}{\sqrt{2\pi\nu^2(t)}} \exp\left[\frac{-(y-\mu(t))^2}{2\nu^2(t)}\right], \tag{86}$$

with

$$\mu(t) = \frac{A}{\lambda}\left(e^{\lambda t} - 1\right) + y_0 e^{\lambda t} \quad \text{and} \quad \nu^2(t) = \frac{c^2}{2\lambda}\left(e^{2\lambda t} - 1\right), \tag{87}$$

where we have assumed the (general, possibly biased) initial condition $p(y,0) = \delta(y - y_0)$ corresponding to starting all paths of (84) at $y(0) = y_0$. Note that the expressions of (87) for mean and variance hold for both positive and negative λ, and that as $\lambda \to 0$, they approach the corresponding expressions for the constant drift case:

$$\mu(t)\mid_{\lambda=0} = At + y_0 \quad \text{and} \quad \nu^2(t)\mid_{\lambda=0} = c^2 t\,. \tag{88}$$

Assuming that the upper threshold $y = +z$ represents the correct choice, the probabilities of correct and incorrect choices being made upon interrogation at time t are therefore:

$$\mathcal{P}(\text{correct}) = 1 - \text{ER} = \int_0^\infty p(y,t)\,dy \quad \text{and} \quad \mathcal{P}(\text{incorrect}) = \text{ER} = \int_{-\infty}^0 p(y,t)\,dy\,. \tag{89}$$

Using the change of variables

$$u = \frac{y-\mu}{\sqrt{2\nu^2}},$$

and the expressions (86) for p, the first of these integrals becomes

$$\mathcal{P}(\text{correct}) = \int_{-\frac{\mu}{\sqrt{2\nu^2}}}^\infty \frac{1}{\sqrt{\pi}} e^{-u^2}\,du = \frac{1}{2}\left[1 + \text{erf}\left(\frac{\mu}{\sqrt{2\nu^2}}\right)\right], \tag{90}$$

and consequently we also have

$$\mathcal{P}(\text{incorrect}) = \text{ER} = \frac{1}{2}\left[1 - \text{erf}\left(\frac{\mu}{\sqrt{2\nu^2}}\right)\right]. \tag{91}$$

4.2.1 Minimizing error rate for unbiased choices

We first consider the case of unbiased initial data, appropriate to choice tasks with alternatives of equal probability. Using (87) with $y_0 = 0$, the argument of the error functions in (90-91) takes the form

$$\frac{\mu}{\sqrt{2\nu^2}} \stackrel{\text{def}}{=} f(\lambda; A, c) = \frac{A}{c}\sqrt{\frac{(e^{\lambda t} - 1)}{\lambda(e^{\lambda t} + 1)}}\,. \tag{92}$$

Since $\text{erf}(\cdot)$ is a monotonically increasing function of its argument on $(-\infty, \infty)$, the probability of making a correct decision will be maximized (and the error rate minimized), by selecting the maximum admissible value of this expression. The appropriate constraints are to fix A and t and maximize (92) over $\lambda \in (-\infty, +\infty)$. We claim that the unique (global) maximum is achieved for $\lambda = 0$:

$$\lim_{\lambda \to 0} f(\lambda; A, c) = \frac{A}{c}\sqrt{\frac{t}{2}}\,. \tag{93}$$

To prove this it suffices to show that $\frac{\partial f}{\partial \lambda} = 0$ at $\lambda = 0$ and $\frac{\partial f}{\partial \lambda}$ is strictly positive (resp., negative) for $\lambda < 0$ (resp., $\lambda > 0$). We compute

$$\frac{\partial f}{\partial \lambda} = \frac{A}{2c}\sqrt{\frac{\lambda(e^{\lambda t}+1)}{e^{\lambda t}-1}}\left[\frac{2\lambda t e^{\lambda t} - e^{2\lambda t} + 1}{\lambda^2(e^{\lambda t}+1)^2}\right] \stackrel{\text{def}}{=} \frac{A}{2c} F(\lambda, t)\,(2\lambda t e^{\lambda t} - e^{2\lambda t} + 1)\,, \tag{94}$$

where $F(\lambda, t)$ is a bounded positive quantity for $\lambda \neq 0$, $t > 0$ and the expression as a whole vanishes ($\sim -\lambda t^{5/2}$) at $\lambda = 0$. The final quantity in parentheses in (94) is positive (resp. negative) for $\lambda < 0$ (resp. $\lambda > 0$), as required. We conclude that the optimal strategy is to set $\lambda = 0$.

4.2.2 Minimizing error rate for biased choices

We now repeat the calculations allowing biased initial data and unequal prior probabilities for the two alternatives. As in our review of SPRT in Section 2, let Π denote the probability of a stimulus corresponding to the upper threshold, with drift $+A$, and $1 - \Pi$ correspond to $-A$. Letting $\text{ER}(\pm) = \text{ER}(\pm A, \lambda, c, x_0)$ denote the error rates in the two cases, the net error rate is:

$$\text{NER} = \Pi\,\text{ER}(+) + (1 - \Pi)\,\text{ER}(-)\,. \tag{95}$$

ER(+) is given by substitution of the general ($y_0 \neq 0$) expressions of (87) into (91). To obtain ER(−) we observe that the reflection transformation $y \mapsto -y$ takes sample paths of (84) with $A > 0$ to those for $A < 0$; we may thus simply substitute $-y_0$ for y_0 in (87), obtaining:

$$\text{NER} = \frac{1}{2}\left[1 - \Pi\,\text{erf}(f^+) - (1 - \Pi)\,\text{erf}(f^-)\right]\,, \tag{96}$$

where

$$f^{\pm} = f^{\pm}(\lambda, y_0; A, c) = \frac{A}{c}\sqrt{\frac{(e^{\lambda t}-1)}{\lambda(e^{\lambda t}+1)}} \pm \frac{y_0}{c}\sqrt{\frac{\lambda e^{2\lambda t}}{e^{2\lambda t}-1}}\,, \tag{97}$$

and, for future use:

$$\begin{aligned}
\frac{\partial f^{\pm}}{\partial y_0} &= \pm\frac{1}{c}\sqrt{\frac{\lambda e^{2\lambda t}}{e^{2\lambda t}-1}} \stackrel{\text{def}}{=} \pm \partial f_{y_0}\,, \\
\frac{\partial f^{\pm}}{\partial \lambda} &= \frac{A}{2c} F(\lambda, t)\,(2\lambda t e^{\lambda t} - e^{2\lambda t} + 1) \pm \frac{y_0}{2c\sqrt{\lambda}}\left(\frac{e^{\lambda t}(e^{2\lambda t} - 1 - 2\lambda t)}{(e^{2\lambda t}-1)^{\frac{3}{2}}}\right) \stackrel{\text{def}}{=} \partial f_{\lambda_1} \pm \partial f_{\lambda_2}\,.
\end{aligned} \tag{98}$$

To minimize the net error rate we compute the partial derivatives of (96):

$$\frac{\partial}{\partial y_0}(\text{NER}) = \frac{1}{\sqrt{\pi}}\left[-\Pi \exp[-(f^+)^2] + (1 - \Pi)\exp[-(f^-)^2]\right]\partial f_{y_0}\,, \tag{99}$$

$$\begin{aligned}
\frac{\partial}{\partial \lambda}(\text{NER}) = -\frac{1}{\sqrt{\pi}}\Big[&\big(\Pi \exp[-(f^+)^2] + (1 - \Pi)\exp[-(f^-)^2]\big)\,\partial f_{\lambda_1} \\
&+ \big(\Pi \exp[-(f^+)^2] - (1 - \Pi)\exp[-(f^-)^2]\big)\,\partial f_{\lambda_2}\Big]\,.
\end{aligned} \tag{100}$$

Setting (99) equal to zero and using (97) we obtain

$$\exp[(f^+)^2 - (f^-)^2] = \frac{\Pi}{1-\Pi} \;\Rightarrow\; \frac{4Ay_0 e^{\lambda t}}{c^2(e^{\lambda t}+1)} = \log\left(\frac{\Pi}{1-\Pi}\right), \tag{101}$$

and substituting (101) into (100) and using the properties of ∂f_{λ_1} derived directly below equation (94), we conclude that

$$\lambda = 0 \quad \text{and} \quad y_0 = \frac{c^2}{2A}\log\left(\frac{\Pi}{1-\Pi}\right) \tag{102}$$

at the critical point.

To check that this is indeed a minimum we compute the Hessian matrix of second partial derivatives at (102), obtaining

$$\begin{aligned}
\frac{\partial^2}{\partial y_0^2}(\text{NER}) &= \frac{2}{\sqrt{\pi}}\Pi \exp[-(f^+)^2]\left(f^+ + f^-\right)[\partial f_{y_0}]^2 = \frac{2}{\sqrt{\pi}}\Pi\exp[-(f^+)^2]\frac{A}{\sqrt{2tc^3}}, \\
\frac{\partial^2}{\partial \lambda^2}(\text{NER}) &= \frac{2}{\sqrt{\pi}}\Pi \exp[-(f^+)^2]\left(f^+ + f^-\right)[\partial f_{\lambda_2}]^2 = \frac{2}{\sqrt{\pi}}\Pi\exp[-(f^+)^2]\frac{Ay_0^2 t^{\frac{3}{2}}}{4\sqrt{2}c^3}, \\
\frac{\partial^2}{\partial y_0 \partial \lambda}(\text{NER}) &= \frac{2}{\sqrt{\pi}}\Pi \exp[-(f^+)^2]\left(f^+ + f^-\right)[\partial f_{y_0}\partial f_{\lambda_2}] = \frac{2}{\sqrt{\pi}}\Pi\exp[-(f^+)^2]\frac{Ay_0\sqrt{t}}{2\sqrt{2}c^3}
\end{aligned} \tag{103}$$

The second variation is therefore positive semidefinite, vanishing only along the line

$$y_0 = \frac{c^2}{2A}\log\left(\frac{\Pi}{1-\Pi}\right)\left[1 - \frac{\lambda t}{2}\right],$$

and direct computations of NER (for all parameters we sampled) show that the point (102) is indeed a minimum along this line.

4.3 ERs for the bounded diffusion model

Here we describe interrogation protocol ERs for a variant of the models considered above, in which trajectories $x(t)$ are restricted to remain within the interval $[-z, z]$. This situation approximates the limits imposed by the finite dynamic range of the firing rates of neurons [1]; note that the no-flux boundaries used here play a completely different role from the absorbing thresholds used to model the free response protocol. For simplicity, we consider only the constant drift-diffusion model, rescaled without loss of generality so that $c = 1$:

$$dx = A\,dt + dW. \tag{104}$$

To simplify the following calculations, we set the boundaries at 0 and $2z$ and the (symmetric) initial condition $x(0) = z$. We first show how to calculate the probability distribution $p(x,t)$ of a solution occupying the point x at time t. The ER is then found by integration of this probability distribution over the appropriate range.

The probability distribution $p(x,t)$ for solutions of (104) satisfies the forward Kolmogorov or Fokker-Planck equation

$$\frac{\partial p(x,t)}{\partial t} = -A\frac{\partial p(x,t)}{\partial x} + \frac{1}{2}\frac{\partial^2 p(x,t)}{\partial x^2}, \tag{105}$$

and the assumption that $x \in (0, 2z)$ implies the following no-flux boundary condition:

$$-Ap(x,t) + \frac{1}{2}\frac{\partial p(x,t)}{\partial x} = 0, \text{ at } x = 0 \text{ and } x = 2z\,. \tag{106}$$

To solve (105) we separate variables [35] and seek a solution of the form

$$p(x,t) = \sum_{j=1}^{\infty} a_j(t)\phi_j(x)\,; \tag{107}$$

obtaining the following eigenvalue problem

$$\frac{1}{2}\phi'' - A\phi' + \lambda\phi = 0\,; \quad -2A\phi(0) + \phi'(0) = 0 = -2A\phi(2z) + \phi'(2z)\,, \tag{108}$$

and the ODE for the time-dependent coefficients $a_j(t)$:

$$\dot{a}_j = -\lambda_j a_j \;\Rightarrow\; a_j(t) = a_j(0)e^{-\lambda_j t}\,. \tag{109}$$

Applying the boundary conditions to the general solution

$$\phi = e^{(A \pm \sqrt{A^2 - 2\lambda})x} \tag{110}$$

of (108), we find a single eigenvalue $\lambda_0 = 0$ with eigenfunction $\phi_0(x) = e^{2Ax}$ and an infinite set of the form

$$\lambda_j = \frac{j^2\pi^2}{8z^2} + \frac{A^2}{2}\,,\ \phi_j(x) = e^{Ax}\left[\cos\left(\frac{j\pi x}{2z}\right) + \frac{2Az}{j\pi}\sin\left(\frac{j\pi x}{2z}\right)\right]. \tag{111}$$

Hence, from (107), the general solution of the Fokker-Planck equation may be written as

$$p(x,t) = a_0(0)e^{2Ax} + \sum_{j=1}^{\infty} a_j(0)e^{-\lambda_j t}\, e^{Ax}\ \left[\cos\left(\frac{j\pi x}{2z}\right) + \frac{2Az}{j\pi}\sin\left(\frac{j\pi x}{2z}\right)\right]. \tag{112}$$

The coefficients $a_j(0)$ are obtained from the initial probability distribution $p(x,0) = p_0(x)$. To compute them, it is convenient to use a weighted inner product with respect to which the (non-normalized) eigenfunctions (111) are orthogonal. Upon multiplication by e^{-2Ax} the non self-adjoint boundary value problem (108) becomes a regular Sturm-Liouville problem [35]:

$$(e^{-2Ax}\phi')' + 2\lambda e^{-2Ax}\,\phi = 0\,, \tag{113}$$

and hence the eigenfunctions are pairwise orthogonal with respect to the weighted inner product:

$$(\phi_j, \phi_k)_A = \int_0^{2z} \phi_j(x)\,\phi_k(x)\,e^{-2Ax}\,dx = c_k\delta_{jk}\,,\ \text{for } j,k = 0,1,2,\ldots\,, \tag{114}$$

with normalization constants

$$c_0 = \frac{e^{4Az} - 1}{2A}\,,\ \text{and}\ \ c_k = z\left(1 + \frac{4z^2A^2}{k^2\pi^2}\right)\ \text{for } k \geq 1\,. \tag{115}$$

Setting $t = 0$ in (112), equating to $p_0(x)$, and taking inner products, we therefore obtain

$$a_j(0) = \frac{(p_0, \phi_j)_A}{c_j}\,, \text{ for } j \geq 0\,. \tag{116}$$

Now as $t \to \infty$, the terms in the sum of (112) all decay to zero and $p(x,t)$ approaches the equilibrium probability distribution $p_\infty(x) = a_0(0)e^{2Ax}$, so for normalized initial data $\int p_0(x)dx = 1$ it must follow that

$$\int_0^{2z} a_0(0)e^{2Ax}dx = 1 \;\Rightarrow\; a_0(0) = \frac{1}{c_0} = \frac{2A}{e^{4Az}-1}\,. \tag{117}$$

For the delta function initial condition $p_0(x) = \delta(x-z)$, the remaining coefficients for $j \geq 0$ may be computed directly from (116) as:

$$a_j(0) = \frac{e^{-Az}\left[\cos\left(\frac{j\pi}{2}\right) + \frac{2Az}{j\pi}\sin\left(\frac{j\pi}{2}\right)\right]}{z\left(1+\frac{4z^2A^2}{j^2\pi^2}\right)} = \frac{e^{-Az}\left[(-1)^{\frac{j}{2}}\left(\frac{1+(-1)^j}{2}\right) + \frac{2Az}{j\pi}(-1)^{\frac{j-1}{2}}\left(\frac{1-(-1)^j}{2}\right)\right]}{z\left(1+\frac{4z^2A^2}{j^2\pi^2}\right)}\,. \tag{118}$$

Finally, the ER at a fixed time t is computed in a manner analogous to (89) by integrating (112):

$$\text{ER} = \int_0^z p(x,t)\,dx = \frac{1}{1+e^{2Az}} + \sum_{j=1}^{\infty} a_j(0)e^{-\lambda_j t}\,\frac{2ze^{Az}\sin\left(\frac{j\pi}{2}\right)}{j\pi}. \tag{119}$$

Note from the form of the equilibrium probability density $p_\infty(x)$ given above that, unlike for the unbounded constant drift (i.e., $\lambda = 0$) diffusion model, the ER for asymptotically long interrogation times is nonzero.

For the sake of computational efficiency, we suggest the following simple numerical scheme to calculate the density $p(x,t)$ and the resulting ER. The probability distribution is taken to be Gaussian (as for unbounded diffusion) until a time $t = t^*$ when 10^{-6} (e.g.) of the mass lies outside $[0, 2z]$. For $t > t^*$, the above expression is used with $a_j(0)$ obtained from (117), (118), and with the series truncated at J chosen such that the error of approximating the Gaussian $N(x, t = t^*)$ by probability distribution $p_J(x, t = t^*)$ of (112) with J terms in the sum is less than 10^{-6}, i.e.:

$$\int_0^{2z} \left(N(x, t = t^*) - p_J(x, t = t^*)\right)^2 dx < 10^{-6}\,.$$

This gives rise to the density shown in Fig. 9.

5 Variable gain in drift-diffusion and O-U processes

We end this report by considering a related optimization strategy for decision tasks in which the drift (signal strength) and diffusion constant (noise strength) terms vary in time. Thus, we ask how the gain applied to inputs to a decision unit might be chosen to minimize interrogation protocol error rates or to speed forced response decisions at a fixed error rate, all in the presence of changing signal-to-noise ratios. We start with a pure drift-diffusion case and move on to O-U processes. We end by showing that, with optimal gain, both cases reduce to drift-diffusion, as the SPRT predicts. This material is developed in greater detail, and the variable gain parameter related to the dynamics of the modulatory brain nucleus *locus coeruleus*, in [2].

5.1 Decision models with variable gain, signal, and noise

In this section we introduce three models with time dependent signal strength, noise amplitude, and gain. The first is a variant of the pure drift-diffusion process considered above, in which both drift and diffusion terms are multiplied by a common gain $g(t)$:

$$\tau_c dx = g(t)[A(t)\,dt + c(t)\,dW_t] \text{ ((pure) drift-diffusion model) }. \tag{120}$$

The time constant τ_c is introduced for consistency with the models below, and we only consider the case of unbiased initial data $x(0) = 0$.

Next we introduce two decision models, both in wide use, for the mean activity of pairs of mutually inhibiting neural populations. Each population making up such a pair accumulates evidence for one of the two possible stimuli. The first system, the leaky integrator *connectionist* model [36, 9], is:

$$\tau_c dx_1 = \left[-x_1 - \beta f_{g(t)}(x_2) + a_1(t)\right] dt + \frac{c(t)}{\sqrt{2}} dW_t^1 \tag{121}$$

$$\tau_c dx_2 = \left[-x_2 - \beta f_{g(t)}(x_1) + a_2(t)\right] dt + \frac{c(t)}{\sqrt{2}} dW_t^2 \ , \tag{122}$$

where the state variables $x_j(t)$ denote the mean input currents to cell bodies of the jth neural population, the integration implicit in the differential equations modelling temporal summation of dendritic synaptic inputs ([37] and references therein). Additionally, the parameter β sets the strength of mutual inhibition via population firing rates $f_{g(t)}(x_j(t))$, where $f_{g(t)}(\cdot)$ is the sigmoidal 'activation' (or 'frequency-current' or neural 'input-output') function to be described shortly. The stimulus signal received by each population is $a_j(t)$, and the noise terms polluting this signal are $c(t)dW_t^j$, where $c(t)$ sets r.m.s. noise strength and the (independent) increments dW_t^j are as above. Finally, the time constant τ_c reflects the rate at which neural activities decay in the absence of inputs and respond to input changes.

Under the free-response paradigm a decision is made and the response initiated when the firing rate $f_{g(t)}(x_j)$ of either population first exceeds a preset threshold z_j; it is normally assumed that $z_1 = z_2 = z$. For the interrogation protocol, the population with greatest activity x_j (and hence also firing rate) at the interrogation time t determines the decision. We also assume that activities decay to zero after response and prior to the next trial, so that the initial conditions for (121-122) are $x_j(0) = 0$.

The subscript in $f_{g(t)}(\cdot)$ indicates dependence on the time-varying gain, or sensitivity, $g(t)$ of the neural populations: gain sets the slope of the activation function. For example, the logistic function

$$f_{g(t)}(x) = \frac{1}{1 + \exp\left(-4g(t)\,(x - b)\right)} = \frac{1}{2}\left[1 + \tanh\left(2g(t)(x - b)\right)\right] \tag{123}$$

has maximal slope $g(t)$. While this specific form is not required for the results derived below, we do assume that $f_{g(t)}$ takes its time-dependent maximal slope $g(t)$ at some time-independent point, as for (123).

As already mentioned, the connectionist model describes the time evolution of current inputs. A second model is derived in [38], cf. [39, 40, 41], in which the firing rates of neural populations are themselves integrated over time. The version of this *firing rate* model that we study here is:

$$\tau_c dy_1 = \left[-y_1 + f_{g(t)}\left(-\beta y_2 + a_1(t)\right)\right] dt + g(t)\frac{c(t)}{\sqrt{2}} dW_t^1 \tag{124}$$

$$\tau_c dy_2 = \left[-y_2 + f_{g(t)}\left(-\beta y_1 + a_2(t)\right)\right] dt + g(t)\frac{c(t)}{\sqrt{2}} dW_t^2 \ . \tag{125}$$

Here, the y_j are the firing rates of population j and other terms are as above, and we assume that the strength of firing rate fluctuations in response to noise in inputs scales with $g(t)$ (i.e., with the maximal sensitivity of firing rates to the deterministic component of the input). As above, we take initial conditions $y_j(0) = 0$. In the interrogation protocol, the decision is again that which corresponds to the greatest firing rate y_j at the interrogation time. Threshold-crossing in the free-response case is detected directly via $y_j = z_j$.

Note that the firing rate model (124-125) is a standard two-unit recurrent neural network with additive noise [42], and that the main difference between the connectionist and firing rate models is whether all of the deterministic inputs, or just the activity of the opposing population, appear inside the function $f_{g(t)}(\cdot)$. See [2], cf. [37], for more on the relationship between these models.

5.2 One dimensional reductions and linear filters

As discussed above and in [9], in the forced response (interrogation) protocol, the choice $j =$ 1 or 2 is made according to which of the two neural populations has the greatest activity or firing rate at interrogation time t. Therefore, knowledge of the difference

$$y(t) \ \stackrel{\triangle}{=} \ y_1(t) - y_2(t) \quad \text{or} \quad x_c(t) \ \stackrel{\triangle}{=} \ x_1(t) - x_2(t) \tag{126}$$

determines the outcome and reduction of the original two-dimensional problem to a single variable does not *inherently* imply any loss in accuracy. For example, if the difference in firing rates is described by a time-dependent probability density $p(y,t)$ (whose distribution represents variability across behavioral trials), then the error rate at interrogation time t is

$$ER = \int_0^\infty p(y,t)dy \tag{127}$$

if alternative 2 was presented (that is, if $a_2 > a_1$ for $t > t_s$), and

$$ER = \int_{-\infty}^0 p(y,t)dy \tag{128}$$

if alternative 1 was presented. Similar conclusions hold for the connectionist model.

For the free choice protocol the situation is more subtle. The single variable x or y is sufficient to characterize the decision only if the probability density of solutions to (124-125) or (121-122) has approximately collapsed along a one-dimensional 'decision manifold.' Below we will simply assume that this collapse has occurred; however, [1, 2] demonstrate that this assumption holds for fairly broad sets of parameters.

To derive equations for the differences introduced in (126), we linearize the activation functions around the point where they take their maximal slope. For (123), this gives

$$f_{g(t)}(x) \approx \frac{1}{2} + g(t)(x - b) \ , \tag{129}$$

an approximation which we use below. Substituting this into Eqns. (121-122) and subtracting gives the following equation for the difference $x_c \equiv x_1 - x_2$:

$$\tau_c dx_c = [-x_c + \beta g(t) x_c + a(t)]\, dt + c(t) dW_t \qquad \text{(connectionist model)} \ ; \tag{130}$$

similarly, for the difference $y \equiv y_1 - y_2$ Eqns. (124-125) give

$$\tau_c dy = [-y + g(t)\,(\beta y + a(t))]\, dt + g(t)c(t) dW_t \quad \text{(firing rate model)} \ . \tag{131}$$

Eqn. (120) and the one-dimensional reductions of the connectionist and firing rate equations (130) and (131) are Ornstein-Uhlenbeck processes, (affine-) linear in the activities x, x_c, and y and in the input

$$\underbrace{B(t)}_{input} = \underbrace{a(t)}_{signal} + \underbrace{c(t)\frac{dW_t}{dt}}_{noise} \ . \tag{132}$$

We may explicitly solve all these SDEs, for a given realization of the Wiener W_s, $s \in [0, t]$, to obtain respectively

$$x(t) = \int_0^t \frac{g(s)a(s)}{\tau_c} ds + \int_0^t \frac{g(s)c(s)}{\tau_c} dW_s \tag{133}$$

for the drift diffusion model,

$$x_c(t) = \int_0^t \frac{a(s)}{\tau_c} \exp\left(\frac{1}{\tau_c}\int_s^t [\beta g(s') - 1]\, ds'\right) ds + \int_0^t \frac{c(s)}{\tau_c} \exp\left(\frac{1}{\tau_c}\int_s^t [\beta g(s') - 1]\, ds'\right) dW_s \tag{134}$$

for the connectionist model, and

$$y(t) = \int_0^t \frac{a(s)g(s)}{\tau_c} \exp\left(\frac{1}{\tau_c}\int_s^t [\beta g(s') - 1]\, ds'\right) ds + \int_0^t \frac{c(s)g(s)}{\tau_c} \exp\left(\frac{1}{\tau_c}\int_s^t [\beta g(s') - 1]\, ds'\right) dW_s \tag{135}$$

for the firing rate model. Here, dW_s is an increment of a Wiener process as above, and we have assumed unbiased initial data $x(0) = y(0) = z(0) = 0$. These expressions all take the form

$$w(t) = \int_0^t K(t,s)a(s) ds + \int_0^t K(t,s)c(s) dW_s \,, \tag{136}$$

and so we conclude that (133-135) all compute linear filters of their inputs.

At any fixed time t, $w(t)$ is a gaussian-distributed random variable with mean $\int_0^t K(t,s)a(s)$ and variance $\int_0^t K^2(t,s)c^2(s)ds$. Using this fact, after a change of variables the error rate expression (128) becomes

$$\text{ER} = \frac{1}{2}\left[1 - \text{erf}\left(\frac{\left|\int_0^t K(t,s)a(s)\right|}{\int_0^t K^2(t,s)c^2(s)ds}\right)\right] \ . \tag{137}$$

5.3 Optimal signal discrimination in the one-dimensional models

5.3.1 Optimal statistical tests

Given only the noisy input function (132), consider the task of discriminating between the presentation of time-dependent signals $a(t)$ and $-a(t)$ (hypotheses 1 and 0, resp.). The likelihood distributions (now themselves time-dependent) that correspond to an increment of input $dB(t) = \pm a(t)dt + c(t)dW_t$ are, analogously to (18),

$$p_0(t)(dB(t)) = \frac{1}{\sqrt{2\pi c^2(t)dt}}\, e^{-(dB(t)+a(t)dt))^2/(2c^2(t)dt)}\,, \tag{138}$$

$$p_1(t)(dB(t)) = \frac{1}{\sqrt{2\pi c^2(t)dt}}\, e^{-(dB(t)-a(t)dt))^2/(2c^2(t)dt)}\,. \tag{139}$$

The corresponding increment of liklihood evidence is, following (11),

$$dI(t) = \log\left(\frac{p_1(dB(t))}{p_0(dB(t))}\right) = k\frac{a(t)}{c^2(t)}\, dB(t)\,, \tag{140}$$

where k (here taken equal to $2\log(e)$) generally depends on the base of the logarithm. Substituting for the definition of $dB(t)$ as an increment of our input, we have the differential equation for the total information $I(t)$ accumulated at time t

$$dI(t) = k\frac{a(t)}{c^2(t)}\left[a(t)\,dt + c(t)\,dW_t\right]\,, \tag{141}$$

which may be integrated to yield:

$$I(t) = \int_0^t k\frac{a^2(s)}{c^2(s)}ds + \int_0^t k\frac{a(s)}{c(s)}dW_s\,. \tag{142}$$

Comparing with Eqn. (136) shows that the optimal filter is

$$K(t,s) = k\frac{a(s)}{c^2(s)}\ : \tag{143}$$

this is the matched filter for white noise which is fundamental in signal processing [43]. Note that, in (141-142) only the signal-to-noise ratio (a/c) appears.

Thus, with correctly chosen gains (and hence optimal, matched filters), all three of the models can perform the Neyman-Pearson test. For the SPRT, the models must implement not only these optimal filters, but also thresholds at appropriate values. For the pure drift-diffusion and firing rate model, this is straightforward (see [2, 1]); however, for in the connectionist case, non-constant thresholds will result from time-varying gain schedules, complicating the situation.

5.3.2 A direct proof that the kernel $K(t,s) = k\frac{a(s)}{c^2(s)}$ is optimal in the interrogation paradigm

As follows from its matched filter property, the linear filter $K(t,s) = k\frac{a(s)}{c^2(s)}$ which computes log likelihood $l(t)$ for inputs with white noise also produces, for all times t, a filtered (and gaussian) version $w(t)$ of the input (Eqn. (136)) with a maximal integrated signal-to-noise ratio

$$F[K;a,c](t) = \frac{\left|\int_0^t K(t,s)a(s)ds\right|}{\sqrt{\mathbb{E}\left(\int_0^t K(t,s)c(s)dW_s\right)^2}} = \frac{\left|\int_0^t K(t,s)a(s)ds\right|}{\sqrt{\int_0^t K^2(t,s)c^2(s)ds}}\,. \tag{144}$$

For completeness, we now demonstrate this directly.

Minimization of the error rate (127) or (128) for (fixed) interrogation at time $t = T$ is achieved by maximizing F over all possible kernels $K(s)$. This problem in the calculus of variations is solved by computing the first and second variations, with respect to K, of the functional F, setting the first to zero to determine a candidate $\bar{K}$ for the optimal K, and evaluating the second at $\bar{K}$ to check that $D_K^2 F$ is negative (semi-) definite. Henceforth we drop explicit reference to the (fixed, arbitrary) interrogation time $t = T$ in the function K and write $K(T,s) = K(s)$. We compute:

$$\begin{aligned}
\frac{\delta F}{\delta K} &= \lim_{\epsilon\to 0}\frac{d}{d\epsilon}F[K+\epsilon\gamma;a,c](T) = \lim_{\epsilon\to 0}\frac{d}{d\epsilon}\left\{\frac{\int_0^T a(s)[K(s)+\epsilon\gamma(s)]\,ds}{\left[2\int_0^T c^2(s)[K^2(s)+2\epsilon g(s)\gamma(s)+\epsilon^2\gamma^2(s)]\,ds\right]^{\frac{1}{2}}}\right\} \\
&= \lim_{\epsilon\to 0}\frac{1}{\sqrt{2}}\left\{\frac{\int_0^T a(s)\gamma(s)\,ds}{[H(T,\epsilon)]^{\frac{1}{2}}} - \frac{\int_0^T a(s)[K(s)+\epsilon\gamma(s)]\,ds\int_0^T c^2(s)[K(s)\gamma(s)+\epsilon\gamma^2(s)]\,ds}{[H(T,\epsilon)]^{\frac{3}{2}}}\right\} \\
&= \frac{\int_0^T a(s)\gamma(s)\,ds\int_0^T c^2(s)K^2(s)\,ds - \int_0^T a(s)K(s)\,ds\int_0^T c^2(s)K(s)\gamma(s)\,ds}{\sqrt{2}\left[\int_0^T c^2(s)K^2(s)\,ds\right]^{\frac{3}{2}}}\,,
\end{aligned} \tag{145}$$

where $H(T,\epsilon) = \int_0^T c^2(s)[K^2(s) + 2\epsilon K(s)\gamma(s) + \epsilon^2\gamma^2(s)]\,ds$. Setting (145) equal to zero and using the fact that the variation $\gamma(s)$ is arbitrary, we conclude that the critical point indeed occurs at $\bar{K}(s) = k\frac{a(s)}{c^2(s)}$, as given by (143).

To compute the second derivative we differentiate the expression within braces in the penultimate step of (145) with respect to ϵ once more, set $\epsilon = 0$, and evaluate the resulting expression at the critical point (143), obtaining:

$$\left.\frac{\delta^2 F}{\delta K^2}\right|_{K=\bar{K}} = -\frac{\int_0^T c^2(s)\bar{K}^2(s)\,ds\int_0^T c^2(s)\gamma^2(s)\,ds - \left(\int_0^T c^2(s)\bar{K}(s)\gamma(s)\,ds\right)^2}{\sqrt{2}\left[\int_0^T c^2(s)\bar{K}^2(s)\,ds\right]^{\frac{3}{2}}} \le 0\,. \tag{146}$$

In the last step we appeal to Schwarz's inequality. This proves that the second variation is negative semidefinite, and vanishes identically only for variations $\gamma(s) = \kappa\bar{K}(s)$ in the direction of $\bar{K}$ (as expected from (143), which contains the arbitrary 'scaling' parameter k).

Substituting (143) into (144) we obtain

$$F[\bar{g};a,c](T) = \sqrt{\frac{1}{2}\int_0^T\frac{a^2(s)}{c^2(s)}\,ds}\,, \tag{147}$$

and using (137), we obtain the minimum possible error rate for interrogation at time t:

$$\text{ER} = \frac{1}{2}\left[1 - \text{erf}\left(\sqrt{\frac{1}{2}\int_0^T \frac{a^2(s)}{c^2(s)}\,ds}\right)\right]. \tag{148}$$

Since the integrand $(a/c)^2$ is non-negative, the error rate continues to decrease or at worst remains constant as T increases.

5.4 Optimal gains for the three models

We now ask what functional form of $g(t)$ optimizes performance for Eqns (133-135), thereby computing optimal gain trajectories for the (reduced) drift-diffusion, connectionist, and firing rate models. The method is to set $K(s) = \bar{K}(s)$ in (136) and comparing the resulting integrands with those in the SDE solutions (133-135).

5.4.1 Pure drift-diffusion model

Comparing (136) with (133), we see that the optimal gain is simply $\bar{K}$:

$$\bar{g}_{dd}(s) = \tau_c \bar{K}(s) = \tau_c k \frac{a(s)}{c^2(s)}\,; \tag{149}$$

thus, there is a continuum of optimal schedules differing only by a multiplicative scale factor.

5.4.2 Connectionist model

Equations (136) and (134) give

$$\tau_c \bar{K}(s) = \tau_c k \frac{a(s)}{c^2(s)} = \exp\left(\frac{1}{\tau_c}\int_s^T \left[\beta \bar{g}_c(s') - 1\right] ds'\right), \tag{150}$$

where $\bar{g}_c$ is the optimal gain for the connectionist model. Taking the log of this expression, differentiating with respect to s, and solving for $\bar{g}_c(s)$, we obtain:

$$\bar{g}_c(s) = \frac{1}{\beta}\left[1 - \tau_c \frac{d}{ds}\log\left(\frac{a(s)}{c^2(s)}\right)\right]. \tag{151}$$

Note that $\bar{g}_c$ is unique and in particular, independent of k and of the interrogation time T. However, $\bar{g}_c$ is not required to be positive, so may not always be physically admissable. The form of $\bar{g}_c$ may be interpreted as follows. When $\left(\frac{a(s)}{c^2(s)}\right)$ is decreasing, $\bar{g}_c(s) > 1/\beta$ and the O-U process (130) is unstable; hence solutions 'run away,' in the direction $x(s)$, emphasizing higher-fidelity information that was previously collected. When $\left(\frac{a(s)}{c^2(s)}\right)$ is increasing, $\bar{g}_c(s) < 1/\beta$, the O-U process is stable, and the linear term in (130) is attractive, thereby discounting previously integrated information in favor of the higher-fidelity input currently arriving.

We note as above that, because the 'output' neural activity is determined by a gain-dependent function of the dynamical variable x in the connectionist model (see text following Eqns. (121-122)), transient gain schedules also adjust the position of free-response thresholds with respect to x. We leave an exploration of this effect, which does not enter the interrogation protocol or affect the firing rate model, for future studies.

5.4.3 Firing rate model

Equations (136) and (135) give

$$\tau_c \bar{K}(s) = \tau_c k \frac{a(s)}{c^2(s)} = \bar{g}_f(s) \exp\left(\frac{1}{\tau_c} \int_s^T \left[\beta \bar{g}_f(s') - 1 \right] ds' \right) . \tag{152}$$

Defining $f(s) = \tau_c k \frac{a(s)}{c^2(s)} e^{\frac{1}{\tau_c}(T-s)}$, differentiating with respect to s, and restricting to positive functions $\bar{g}_f$, a and c^2 (which we justify below), (152) yields

$$\begin{aligned} f'(s) &= \frac{d}{ds}\left[\bar{g}_f(s) \exp\left(\frac{1}{\tau_c} \int_s^T \beta \bar{g}_f(s') ds' \right) \right] \\ &= \bar{g}_f'(s) \exp\left(\frac{1}{\tau_c} \int_s^T \beta \bar{g}_f(s') ds' \right) - \frac{\beta}{\tau_c} \bar{g}_f^2(s) \exp\left(\frac{1}{\tau_c} \int_s^T \beta \bar{g}_f(s') ds' \right) \\ &= \bar{g}_f'(s) \frac{f(s)}{\bar{g}_f(s)} - \frac{\beta}{\tau_c} \bar{g}_f(s) f(s) . \end{aligned} \tag{153}$$

Rewriting (153), we obtain

$$\begin{aligned} \frac{d\bar{g}_f(s)}{ds} &= \frac{\beta}{\tau_c} \bar{g}_f^2(s) + \bar{g}_f(s) \frac{f'(s)}{f(s)} = \frac{\beta}{\tau_c} \bar{g}_f^2(s) + \bar{g}_f(s) \frac{d}{ds} \log\left(f(s) \right) \\ &= \frac{\beta}{\tau_c} \bar{g}_f^2(s) + \bar{g}_f(s) \left[\frac{d}{ds} \log\left(\frac{a(s)}{c^2(s)} \right) - \frac{1}{\tau_c} \right] . \end{aligned} \tag{154}$$

Thus, the condition for optimal gain in the linearized firing rate model is a differential equation, unlike the algebraic relationships for the drift-diffusion and connectionist cases. Note that solutions to (154) initialized at positive values remain positive for all time, since the equation has an equilibrium at $\bar{g}_f = 0$, preventing passage through this point. This justifies our assumption of positive $\bar{g}_f$ above and ensures that the optimum gain is 'physical' this sense. In fact, (154) may be solved explicitly using the integrating factor $I(s) = \exp\left(\int_0^s l(s') ds' \right)$, where $l(s') \triangleq \frac{d}{ds'} \log\left(\frac{a(s')}{c^2(s')} \right) - \frac{1}{\tau_c}$, yielding

$$\bar{g}_f(s) = \frac{\exp\left(\int_0^s l(s') ds' \right)}{\frac{\beta}{\tau_c} \int_0^s \left[\exp\left(\int_0^{s'} l(s'') ds'' \right) \right] ds' + \frac{1}{g(0)}} . \tag{155}$$

The integral equation (152) specifies only an *arbitrary*, positive final condition $\bar{g}_f(T) = k \frac{a(T)}{c^2(T)}$ for (154), since k is itself arbitrary. Any solution of (154) with positive initial condition (as long as it is defined) therefore delivers a member of the continuum of optimal gain functions for the linearized firing rate model. This is in contrast to the unique optimal gain (151) in the connectionist model, and, since the different $\bar{g}_f$ generally have different forms (see below), it also contrasts with the multiplicity of 'scaled' optimal drift-diffusion gain functions (149). The optimality of $\bar{g}_f$ schedules with such different forms follows from the fact that gain multiplies the inputs to the firing rate model (131). For example, optimal gain schedules with $(\beta \bar{g}_f(s) - 1) < 0$ may implement the SPRT even when the signal-to-noise-ratio is constant (see Example 1 below), because discounting of previously integrated evidence is compensated for via weighting incoming evidence by a decreasing function $\bar{g}_f(s)$.

Example 1: We assume constant signal amplitude $a(s) \equiv a$ and constant noise strength $c(s) \equiv 1$. Additionally, we set $\tau_c = 1$ and omit this parameter in this and the next example. Equation (149) gives the family of optimal gain functions for the drift-diffusion model,

$$\bar{g}(s) \equiv ka\,, \tag{156}$$

and Eqn. (151) gives unique optimal gain for the connectionist model

$$\bar{g}_c(s) \equiv \frac{1}{\beta}\,, \tag{157}$$

hence reducing the connectionist to the pure drift-diffusion (i.e., $\lambda = 0$) model. Meanwhile, Eqn. (154) yields the differential equation

$$\frac{d}{ds}\bar{g}_f(s) = \beta\bar{g}_f^2(s) - \bar{g}_f(s)\,. \tag{158}$$

Initial conditions $\bar{g}_f(0) \in [0, 1/\beta]$ decay to the fixed point at $\bar{g}_f = 0$, while for $\bar{g}_f(0) > 1/\beta$, gain functions increase to ∞ (in finite time). The initial condition $\bar{g}_f(0) = 1/\beta$ yields the constant gain function $\bar{g}_f(s) \equiv 1/\beta$, for which the linearized firing rate model again becomes pure drift-diffusion. The distinction with the connectionist model is, of course, that there are other optimal gain functions giving $\lambda \neq 0$. See Fig. 10, which illustrates several optimal functions $\bar{g}_f$ for the case of constant a and c; these include, but are not limited to, the constant value $\bar{g}_f \equiv 1/\beta$. All such $\bar{g}_f$'s yield identical error rates of 0.24 for interrogation at time $T = 2$.

Example 2: We assume now assume that signal amplitude smoothly rises from a low level $a_0 > 0$ (e.g., before stimulus, when only expectation or bias enter neural integrators) to a higher level $\bar{a} + a_0$ (e.g., after stimulus is presented). We use the sigmoidal function $a(s) = a_0 + \frac{\bar{a}}{1+\exp(-4r(\tau-s))}$, so that the increase in signal occurs around time $s = \tau$ with maximum rate r, and additionally, we again take constant noise strength $c(s) \equiv 1$. Then, Eqn. (149) gives

$$\bar{g}(s) \equiv ka(s)\,, \tag{159}$$

and Eqn. (151) yields

$$\bar{g}_c(s) = \frac{1}{\beta}\left[1 - l(s)\right]\,, \tag{160}$$

where the function $l(s) = \frac{d}{ds}\log\left(a_0 + \frac{\bar{a}}{1+\exp(-4r(\tau-s))}\right)$ is a single-peaked 'bump' function. Meanwhile, Eqn. (154) yields the differential equation

$$\frac{d}{ds}\bar{g}_f(s) = \beta\bar{g}_f^2(s) + \bar{g}_f(s)\left[l(s) - 1\right]\,. \tag{161}$$

Solutions $\bar{g}_f(s) > 0$ that lie to the left of $\frac{1}{\beta}[1 - l(s)]$ at any time s decrease toward 0; those that lie to the left increase. While $a(s)$ is increasing, this dividing point is itself further to the left, so that more trajectories increase (temporarily). See Fig. 11, which illustrates different optimal

$\bar{g}_f$ functions. The optimal performance yielded by (all three of) these these functions was 96.2 percent correct; for comparison, the *non-optimal* 'pure drift' gain $\bar{g}_f(s) \equiv 1/\beta$ produces only 87.4 percent correct for the parameters of Fig. 11.

Of special interest are solutions of the type highlighted in Fig. 11 (the lowest-valued optimal $\bar{g}_f(s)$), because such physically plausible gain functions remain bounded. A class of optimal gain functions of this form, determined by their (sufficiently small) initial conditions, will always exist for any given parameters in the logistic a function. We observe that the 'decay-rise-decay' $\bar{g}_f(s)$ dynamical pattern resembles the function that could be produced by dissipating pulses of the neuromodulator norepinephrine delivered to decision areas of the cortex via the locus coeruleus, hence providing a clue that this brainstem organ may be assisting near-optimal decision making. See [2] for more detail.

Acknowledgements

This work was partially funded by the grants NIH P50 MH062196 (Cognitive and Neural Mechanisms of Conflict and Control, Silvio M. Conte Center) and DOE DE-FG02-95ER25238 (P.H.). J.M was supported under a NSF Mathematical Sciences Postdoctoral Research Fellowship, E.B. under a Burroughs-Wellcome Training Grant in Biological Dynamics and by the Princeton Graduate School, and M.G. under a NSF Graduate Fellowship. The authors thank Mark Gilzenrat and Jaime Cisternas for useful contributions and discussions.

References

[1] R. Bogacz, E. Brown, J. Moehlis, P. Hu, P. Holmes, and J.D. Cohen. The physics of optimal decision making: a formal analysis of models of performance in two-alternative forced choice tasks. *Submitted to Psych. Rev.*, 2004.

[2] E. Brown, J. Gao, P. Holmes, R. Bogacz, M. Gilzenrat, and J.D. Cohen. Simple networks that optimize decisions. *Int. J. Bifurcation and Chaos*, to appear, 2004.

[3] D.R.J. Laming. *Information Theory of Choice-Reaction Times*. Academic Press, New York, 1968.

[4] M. Stone. Models for choice-reaction time. *Psychometrika*, 25:251–260, 1960.

[5] R. Ratcliff. A theory of memory retrieval. *Psych. Rev.*, 85:59–108, 1978.

[6] R. Ratcliff, T. Van Zandt, and G. McKoon. Connectionist and diffusion models of reaction time. *Psych. Rev.*, 106 (2):261–300, 1999.

[7] J.D. Schall. Neural basis of deciding, choosing and acting. *Nature Reviews in Neuroscience*, 2:33–42, 2001.

[8] S.C. Cannon, D.A. Robinson, and S. Shamma. A proposed neural network for the integrator of the oculomotor system. *Biological Cybernetics*, 49:127–136, 1983.

[9] M. Usher and J.L. McClelland. On the time course of perceptual choice: The leaky competing accumulator model. *Psych. Rev.*, 108:550–592, 2001.

[10] S. Seung. Amplification, attenuation and integration. In M.A. Arbib, editor, *The Handbook of Brain Theory and Neural Networks*. MIT Press, Cambridge, MA, 2003.

[11] R.H.S. Carpenter and M.L.L. Williams. Neural computation of log likelihood in control of saccadic eye movements. *Nature*, 377:59–62, 1995.

[12] J.I. Gold and M.N Shadlen. Neural computations that underlie decisions about sensory stimuli. *Trends in Cognitive Science*, 5 (1):10–16, 2001.

[13] J.I. Gold and M.N. Shadlen. Banburismus and the brain: decoding the relationship between sensory stimuli, decisions, and reward. *Neuron*, 36:299–308, 2002.

[14] P.W. Glimcher. Decisions, decisions, decisions: Choosing a biological science of choice. *Neuron*, 36:323–332, 2002.

[15] W. Feller. *An introduction to probability theory and its applications*. Wiley, New York, 1957. 2 volumes. Second Edition.

[16] J. Neyman and E.S. Pearson. On the problem of the most efficient tests of statistical hypotheses. *Philos. Trans. Roy. Soc. London Ser. A.*, 231:289–337, 1933.

[17] A. Wald. *Sequential Analysis*. John Wiley & Sons, New York, 1947.

[18] W.A. Wallis. The Statistical Research Group, 1942-1945. *J. Amer. Statist. Assoc.*, 75:320–330, 1980.

[19] G.A. Barnard. Sequential tests in industrial statistics. *J. Roy. Statist. Soc. Suppl.*, 8:1–26, 1946.

[20] M.H. DeGroot. A conversation with George A. Barnard. *Statist. Sci.*, 3:196–212, 1988.

[21] I.J. Good. Studies in the history of probability and statistics. XXXVI. A.M. Turing's statistical work in World War II. *Biometrika*, 66:393–396, 1979.

[22] B.K. Ghosh. *Sequential Tests of Statistical Hypotheses*. Addison-Wesley, Reading, Massachusetts, 1970.

[23] Z. Govindarajulu. *Sequential Statistical Procedures*. Academic Press, New York, 1975.

[24] D. Siegmund. *Sequential Analysis: Tests and Confidence Intervals*. Springer, New York, 1985.

[25] G.B. Wetherill and K.D. Glazebrook. *Sequential Methods in Statistics, Third Edition*. Chapman and Hall, New York, 1986.

[26] B.K. Ghosh and P.K. Sen (eds.). *Handbook of Sequential Analysis*. Marcel Dekker, New York, 1991.

[27] N. Schmitz. *Optimal Sequentially Planned Decision Procedures.* Springer, New York, 1993.

[28] A. Wald and J. Wolfowitz. Optimum character of the sequential probability ratio test. *Ann. Math. Statist.*, 19:326–339, 1948.

[29] E.L. Lehmann. *Testing Statistical Hypotheses.* John Wiley & Sons, New York, 1959.

[30] P. Billingsley. *Proabability and Measure.* Wiley, New York, 1995.

[31] C.W. Gardiner. *Handbook of Stochastic Methods, Second Edition.* Springer, New York, 1985.

[32] D.J. Higham. An algorithmic introduction to numerical simulation of stochastic differential equations. *SIAM Rev.*, 43:525–546, 2001.

[33] M. Abramowitz and I.A. Stegun, eds. *Handbook of Mathematical Functions with Formulas, Graphs, and Mathematical Tables.* Wiley - Interscience, New York, 1984.

[34] J. Spanier and K.B. Oldham. *An Atlas of Functions.* Hemisphere Pub. Corp., Washington, 1987.

[35] W.E. Boyce and R.C. DiPrima. *Elementary Differential Equations and Boundary Value Problems.* Wiley, New York, 1997.

[36] J.L. McClelland. On the time relations of mental processes: An examination of systems of processes in cascade. *Psychological Review*, 86:287–330, 1979.

[37] S. Grossberg. Nonlinear neural networks: principles, mechanisms, and architectures. *Neural Networks*, 1:17–61, 1988.

[38] H. Wilson and J. Cowan. Excitatory and inhibitory interactions in localized populations of model neurons. *Biophys. J.*, 12:1–24, 1972.

[39] J.J. Hopfield. Neurons with graded response have collective computational properties like those of two-state neurons. *Proc. Natl. Acad. Sci. USA*, 82:3088–3092, 1984.

[40] L. Abbott. Firing-rate models for neural populations. In O. Benhar, C. Bosio, P. Del Giudice, and E. Tabat, editors, *Neural Networks: from Biology to High-Energy Physics*, pages 179–196. ETS Editrice, Pisa, 1991.

[41] W. Gerstner and W. Kistler. *Spiking Neuron Models.* Cambridge University Press, 2002.

[42] J. Hertz, A. Krough, and R. Palmer. *Introduction to the Theory of Neural Computation.* Perseus Book Group, New York, 1991.

[43] A. Papoulis. *Signal Analysis.* McGraw-Hill, New York, 1977.

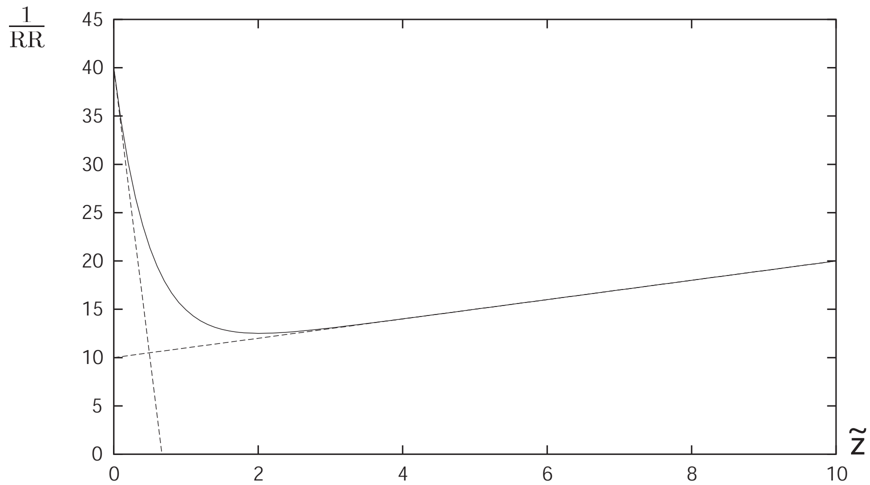

Figure 1: 1/RR vs. $\tilde{z}$ for constant drift-diffusion equation with $\tilde{a} = 1, D = 10, D_p = 20$. The solid line shows the exact result given by (40), while the dashed lines show the small and large $\tilde{z}$ approximations given by (43) and (45).

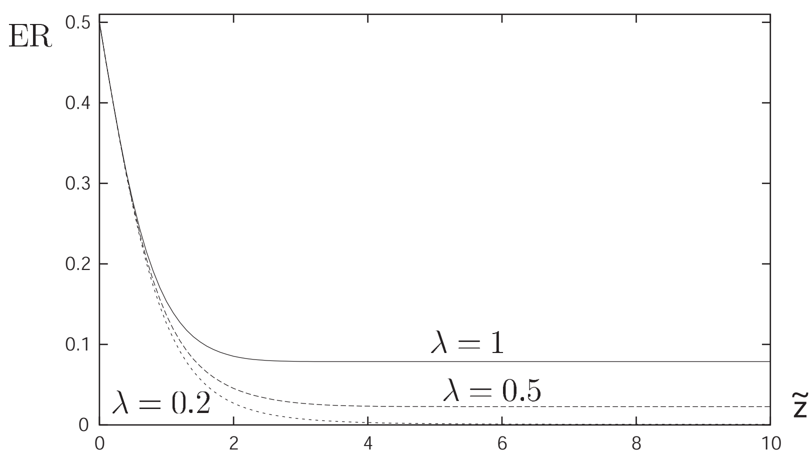

Figure 2: Error rate ER vs. $\tilde{z}$ for $\tilde{a} = 1$ and λ values as shown.

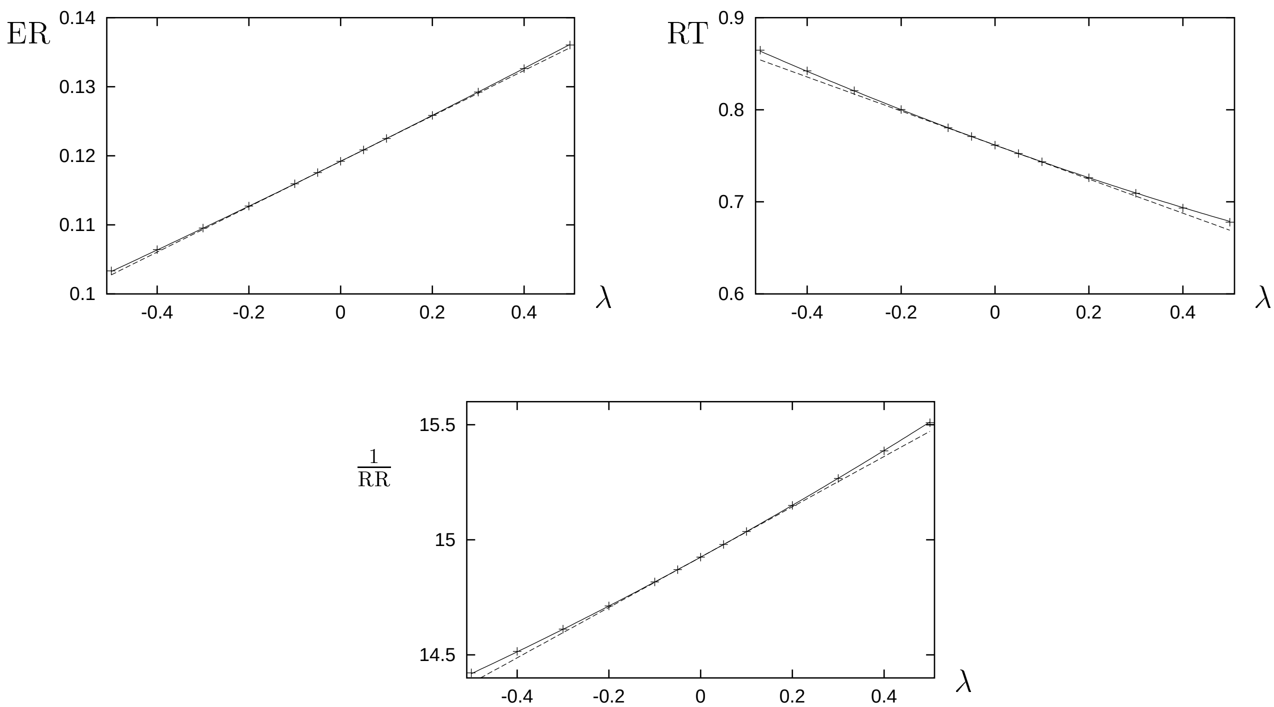

Figure 3: Validity of approximations for $\tilde{z} = 1$, $\tilde{a} = 1$, $D = 10$, and $D_p = 20$. Here the +'s are from the exact formulas (52), (53), and (54), and the solid (resp., dashed) lines are results from (60), (61), and (62) to $\mathcal{O}(\lambda^2)$ (resp., $\mathcal{O}(\lambda)$).

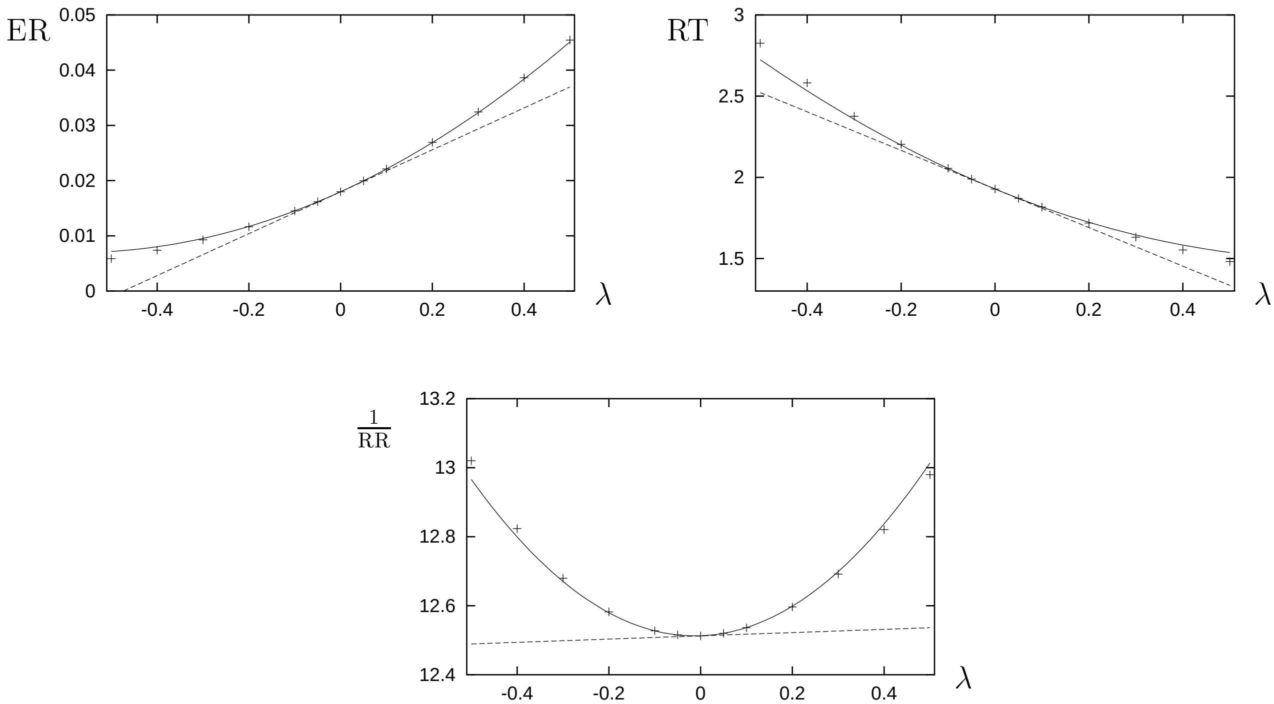

Figure 4: Same as Fig. 3 but with $\tilde{z} = 2$.

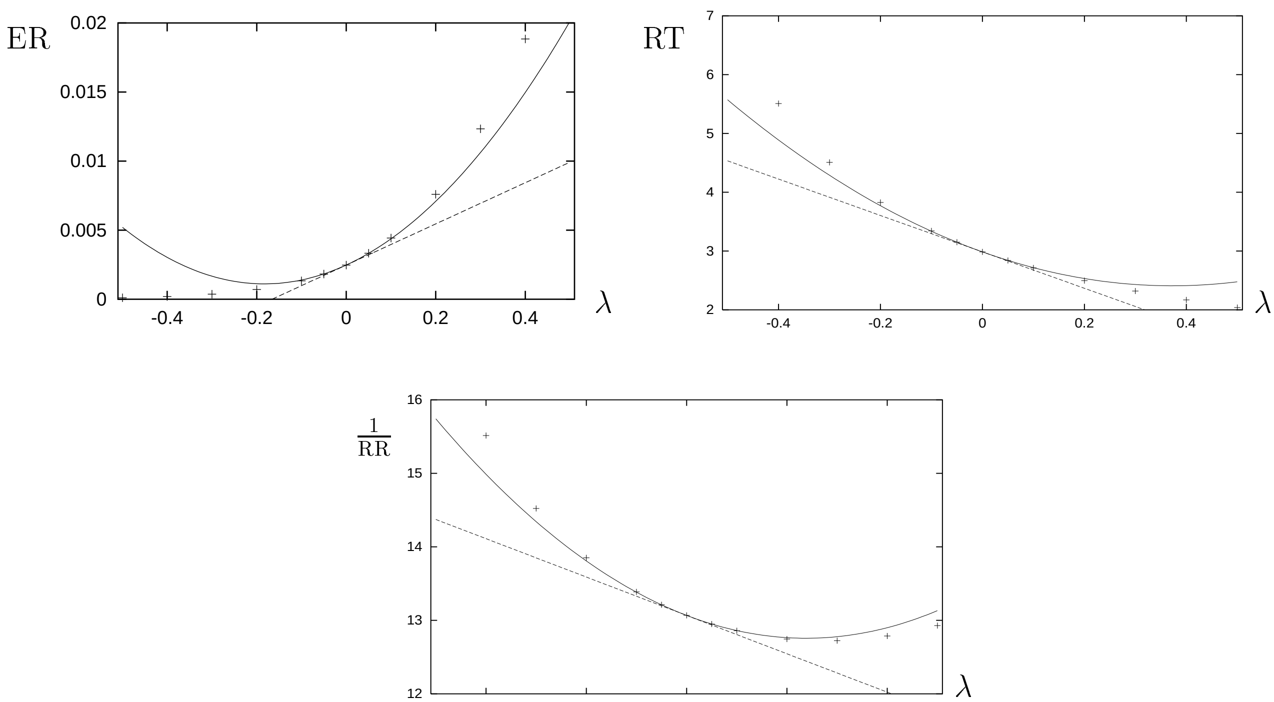

Figure 5: Same as Fig. 3 but with $\tilde{z} = 3$.

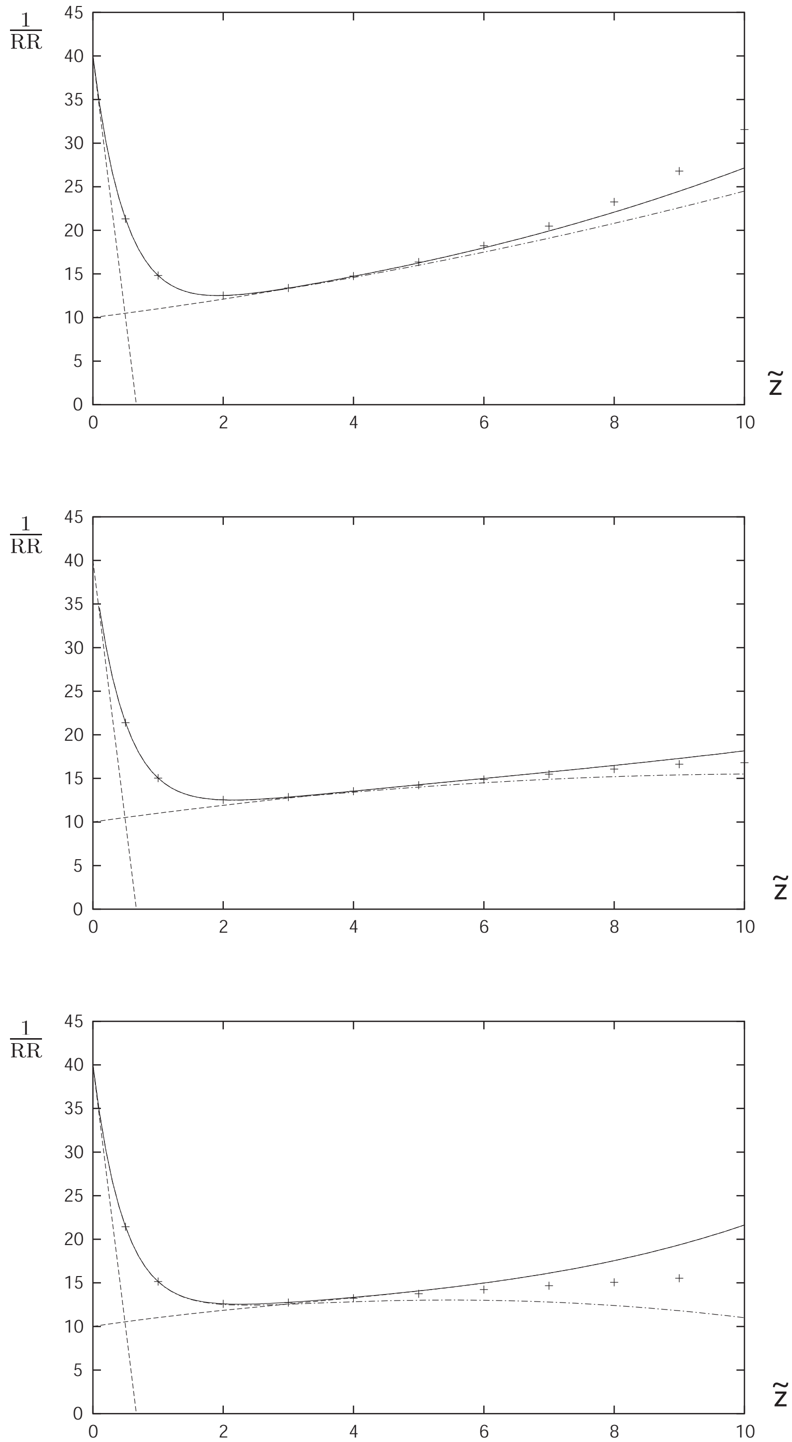

Figure 6: Validity of approximations for $\tilde{a} = 1, D = 10, D_p = 20$. (Top) $\lambda = -0.1$, (middle) $\lambda = 0.1$, (bottom) $\lambda = 0.2$. Here the +'s are from the exact formula (54), and the solid (resp., dot-dashed) lines are results from (62) to $\mathcal{O}(\lambda^2)$ (resp., $\mathcal{O}(\lambda)$). The dashed lines show the small and large $\tilde{z}$ approximations given by (63) and (64).

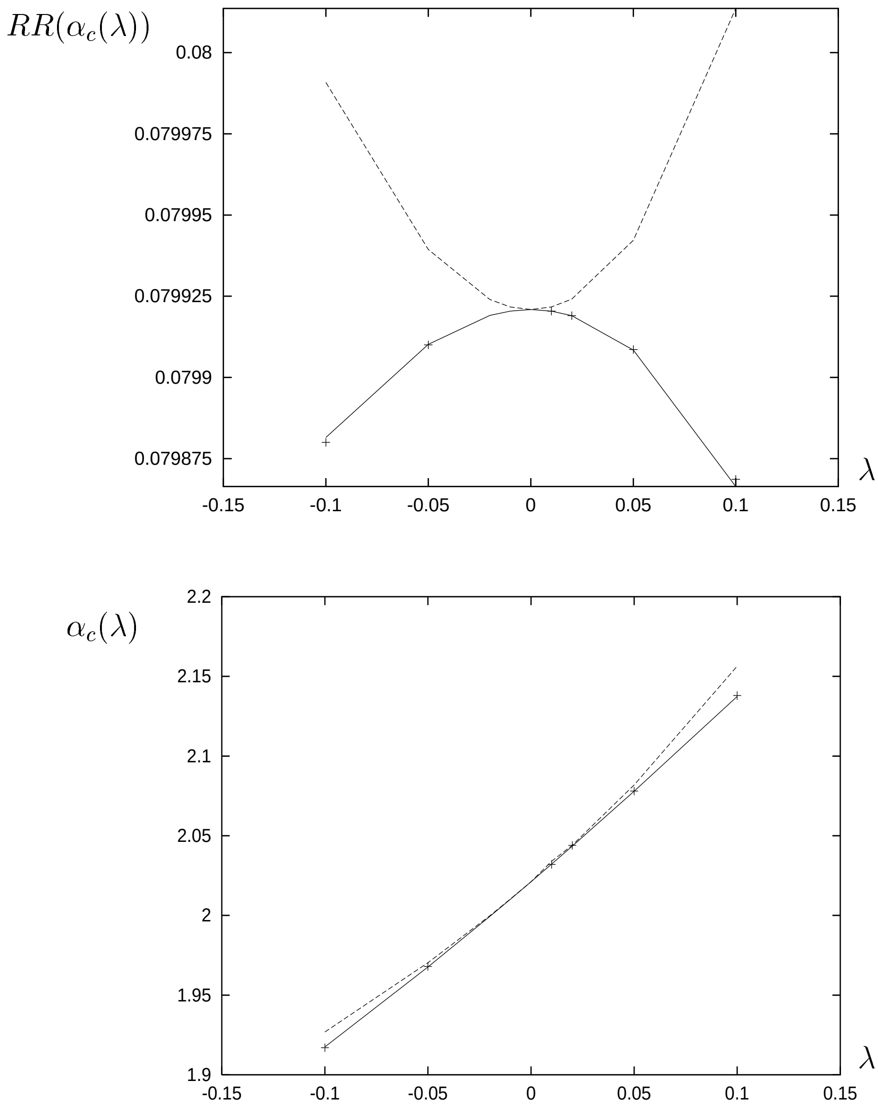

Figure 7: For fixed λ, $\tilde{z}_c(\lambda)$ maximizes RR, giving $RR(\tilde{z}_c(\lambda))$. Results for $\tilde{a} = 1, D = 10, D_p = 20$ where $\tilde{z}_c(\lambda)$ is found from (+'s) exact formula (54), (solid line) equation (62) to $\mathcal{O}(\lambda^2)$, and (dashed line) equation (62) to $\mathcal{O}(\lambda)$.

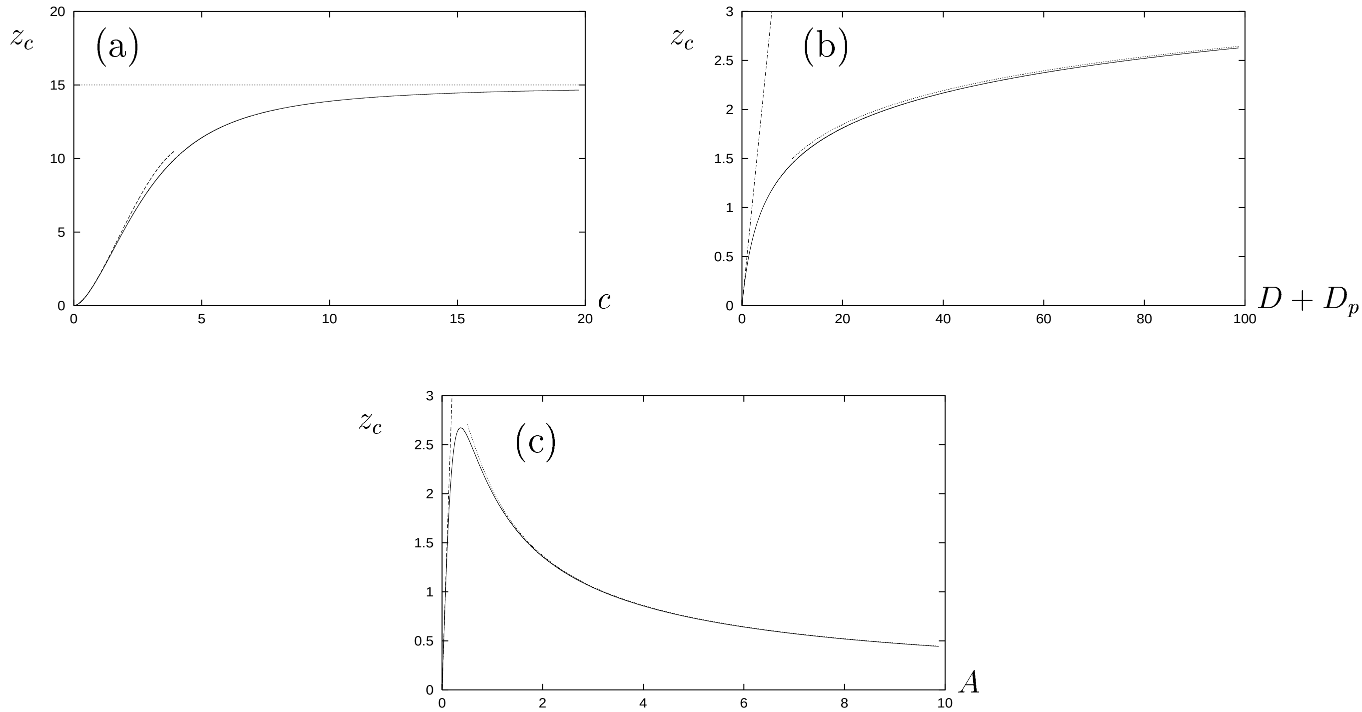

Figure 8: Threshold z_c which optimizes RR as a function of the original system parameters, with (a) $A = 1$, $D + D_p = 30$, (b) $A = 1$, $c = 1$, (c) $c = 1$, $D + D_p = 30$. Approximations for small (resp., large) parameter values are shown as dashed (resp., dotted) lines.

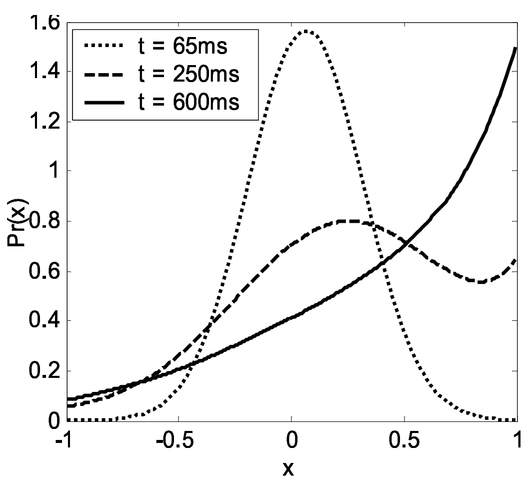

Figure 9: The probability density for solutions to the bounded diffusion model at three times, with parameters $A = z = 1$.

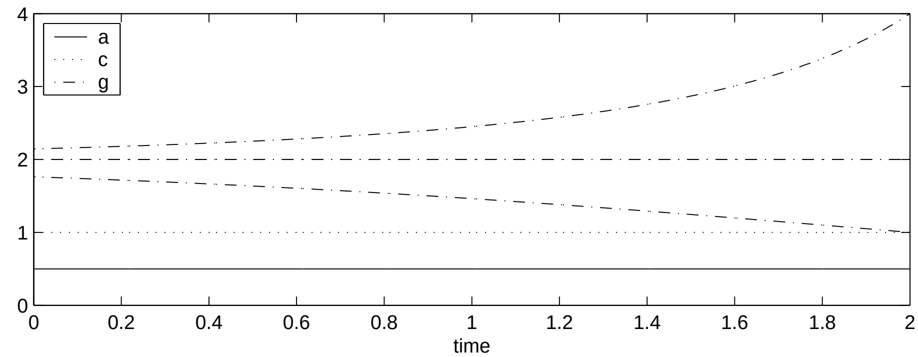

Figure 10: Optimal gain in the firing rate model for constant signal strength $a(s) \equiv 0.5$ (solid line) and constant noise amplitude $c(s) \equiv 1$ (dotted line). Parameters: $T = 2,\ \beta = 0.5$. Three optimal gain functions $\bar{g}_f$ obtained by solving (154) are shown as chain-dotted lines; all of these produced optimal performance with 76.0 percent correct responses (error rate = 0.24). Note that the optimal gain functions include, but are not limited to, $\bar{g}_f(s) \equiv 1/\beta$.

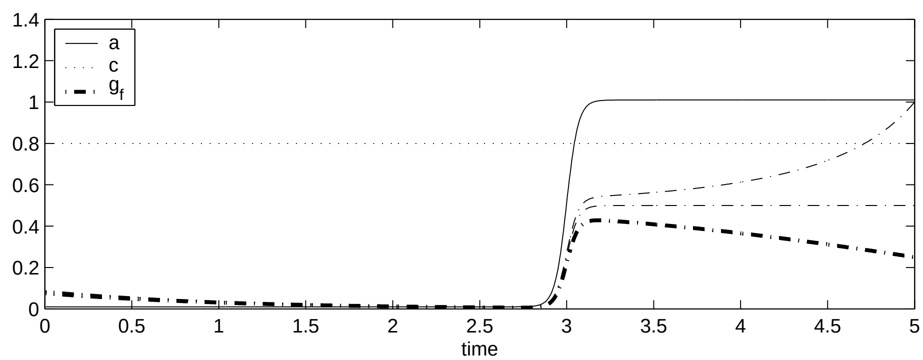

Figure 11: Optimal gain in the firing rate model for sigmoidally increasing signal strength $a(s) = a_0 + \frac{\bar{a}}{1+\exp(-4r(\tau-s))}$ (solid line) and constant noise amplitude $c(s) \equiv 1$ (dotted line). Parameters: $a_0 = 0.01,\ \bar{a} = 1,\ r = 30,\ \tau = 3, T = 5,\ \beta = 2$. Three optimal gain functions $\bar{g}_f$ obtained by solving (154) are shown as chain-dotted lines; all of these produced optimal performance with 96.2 percent correct responses (error rate = 0.038), compared with the non-optimal 87.4 percent correct value for constant $g(s) \equiv 1/\beta$ (not shown). The bold chain-dotted line is an example of an optimal gain function with the decay-rise-decay form discussed in the text.